AD-A280 689

DTIC
S ELECTE
JUN 2 7 1994
F D

Effects of Thickness and Curvature on the Natural
Frequencies of Cylindrical Composite Shells

THESIS

José L. Monteverde E.
Ecuadorian Air Force

AFIT/GAE/ENY/94J-2

94-19394

94 6 24 017

Effects of Thickness and Curvature on the Natural Frequencies of
Cylindrical Composite Shells

THESIS

Presented to the Faculty of the Graduate School of Engineering

of the Air Force Institute of Technology

Air University

In Partial Fulfillment of the

Requirments for the Degree of

Master of Science In Aeronautical Engineering

Jose L. Monteverde
Ecuadorian Air Force

June, 1994

Approved for public release; distribution unlimited.

Acknowledgments

I am deeply indebted to my advisor, Dr. Anthony Palazotto, for all of his help, expertise guidance and considerable patience throughout the completion of this thesis. Also, I would like to thank my thesis commitee members Dr. Peter J. Torvik and Capt. Robert Canfield for their valuable suggestions and advise.

I want to thank my parents for their love and support, for being there and for always believing in me.

Special thanks goes for Rocio, for her understanding (sometimes), support and encouragement during most of the time of my tenure at AFIT.

I save, for last, my deepest apreciation and love for my son Daniel, whose smile and tenderness given me every day, no matter how hard it was, produced a happy ending.

Table of Contents

List of Figures

List of Tables

List of Symbols

Symbol

a	Length in the x direction
b	Length in the y direction
c	System damping
E	Young's Elastic Modulus
F	External applied force
G	Shear Modulus
h	Laminate thickness
k	Stiffness of System
K	Stiffness Matrix
m	Mass of System
M	Consistent Mass Matrix
N	Shape Function Matrix
R	Radius of Curvature
t	time
u	Displacement in the x coordinate direction
v	Displacement in the s coordinate direction
w	Transverse displacement in the z coordinate direction
$w_{,1}$	Slope $\partial w / \partial x$ at the node
$w_{,2}$	Slope $\partial w / \partial s$ at the node

ϕ	Characteristic eigenvector of a system
Φ	Matrix of characteristic eigenvectors
λ	Characteristic eigenvalue of a system
Λ	Matrix of characteristic eigenvalues
ν_{ij}	Poisson's Ratio
ρ	Mass density
ξ	Curvilinear coordinates of the surface
Ω	Domain of the midsurface
Ψ_1	Rotation of the normal to the shell surface in the x direction (about the s axis)
Ψ_2	Rotation of the normal to the shell surface in the s direction (about the x axis)

Abstract

An analytical study is performed to determine the dynamic response, natural frequencies and mode shapes, of deep composite cylindrical shells, including the effect of through the thickness shear strain. The DSHELL finite element program is used to predict the first four natural frequencies and the results are compared to a reference using the Galerkin technique. The program was extended to problems considering simply supported-free boundary conditions. As is well know, the free boundary is rather difficult to represent using the Galerkin technique approach. The mode shapes are created by plotting a surface-contour plot of the eigenvector output from DSHELL.

A linear, free vibration analysis was performed on two composite panels in which damping effects were assumed negligible. The analyzed panels are made of graphite/epoxy (Gr/Ep) material, having different ply orientations. The first panel, used as a baseline in this study, has an arclength, longitudinal length, and radius of curvature of 12 inches, 11 inches, and 12 inches respectively. A $[0^o/-45^o/+45^o/90^o]_s$ ply orientation under the simply supported-free boundary condition was considered. Comparisons between this baseline panel, using DSHELL, with previous holographic experimentation and analytical studies (STAGSC-1 finite element program was previously incorporated) were found to correlate well. The percent difference was observed to be less tha 8% in all cases. Also, it was found that accurate modeling of the composite shell panel was dictated by the natural frequencies and mode shapes. From this study, four nodes have to be positioned per each half sine wave formed in the eigenvectors.

For the second panel, the curvature and the span to thickness ratio were varied in order to measure effects on two ply orientations, $[0^o/90^o]_s$ and $[-45^o/+45^o]_s$, under two boundary conditions, all edges simply supported and simply supported-free. The result showed that, as the shell becomes deeper, the frequency becomes smaller.

Also, findings show that as curvature increases, the natural frequencies for both laminates increases. The effect of increasing the thickness was more evident at the shallower end of the composite shell. The shear effect was evident for small values of span to thickness ratios and large curvature under the two boundary conditions studied. The percent difference between DSHELL and the Galerkin technique was generally less than 10% in all cases compared. For this study, DSHELL proved to be a very useful engineering tool.

List of Symbols

Symbol

a	Length in the x direction
b	Length in the y direction
c	System damping
E	Young's Elastic Modulus
F	External applied force
G	Shear Modulus
h	Laminate thickness
k	Stiffness of System
K	Stiffness Matrix
m	Mass of System
M	Consistent Mass Matrix
N	Shape Function Matrix
R	Radius of Curvature
t	time
u	Displacement in the x coordinate direction
v	Displacement in the s coordinate direction
w	Transverse displacement in the z coordinate direction
$w_{,1}$	Slope $\partial w / \partial x$ at the node
$w_{,2}$	Slope $\partial w / \partial s$ at the node

ϕ	Characteristic eigenvector of a system
Φ	Matrix of characteristic eigenvectors
λ	Characteristic eigenvalue of a system
Λ	Matrix of characteristic eigenvalues
ν_{ij}	Poisson's Ratio
ρ	Mass density
ξ	Curvilinear coordinates of the surface
Ω	Domain of the midsurface
Ψ_1	Rotation of the normal to the shell surface in the x direction (about the s axis)
Ψ_2	Rotation of the normal to the shell surface in the s direction (about the x axis)

Abstract

An analytical study is performed to determine the dynamic response, natural frequencies and mode shapes, of deep composite cylindrical shells, including the effect of through the thickness shear strain. The DSHELL finite element program is used to predict the first four natural frequencies and the results are compared to a reference using the Galerkin technique. The program was extended to problems considering simply supported-free boundary conditions. As is well know, the free boundary is rather difficult to represent using the Galerkin technique approach. The mode shapes are created by plotting a surface-contour plot of the eigenvector output from DSHELL.

A linear, free vibration analysis was performed on two composite panels in which damping effects were assumed negligible. The analyzed panels are made of graphite/epoxy (Gr/Ep) material, having different ply orientations. The first panel, used as a baseline in this study, has an arclength, longitudinal length, and radius of curvature of 12 inches, 11 inches, and 12 inches respectively. A $[0^o/-45^o/+45^o/90^o]_S$ ply orientation under the simply supported-free boundary condition was considered. Comparisons between this baseline panel, using DSHELL, with previous holographic experimentation and analytical studies (STAGSC-1 finite element program was previously incorporated) were found to correlate well. The percent difference was observed to be less tha 8% in all cases. Also, it was found that accurate modeling of the composite shell panel was dictated by the natural frequencies and mode shapes. From this study, four nodes have to be positioned per each half sine wave formed in the eigenvectors.

For the second panel, the curvature and the span to thickness ratio were varied in order to measure effects on two ply orientations, $[0^o/90^o]_S$ and $[-45^o/+45^o]_S$, under two boundary conditions, all edges simply supported and simply supported-free. The result showed that, as the shell becomes deeper, the frequency becomes smaller.

Also, findings show that as curvature increases, the natural frequencies for both laminates increases. The effect of increasing the thickness was more evident at the shallower end of the composite shell. The shear effect was evident for small values of span to thickness ratios and large curvature under the two boundary conditions studied. The percent difference between DSHELL and the Galerkin technique was generally less than 10% in all cases compared. For this study, DSHELL proved to be a very useful engineering tool.

EFFECTS OF THICKNESS AND CURVATURE ON THE NATURAL FREQUENCIES OF CYLINDRICAL COMPOSITE SHELLS

I. Introduction

Composite materials have reached great acceptance in many technological fields. Due to their superior strength-to-weight and stiffness-to-weight ratios compared with traditional alloys, composite materials are ideal for aerospace structure applications.

Composites are typically formed in layers with the high strength properties usually oriented in the in-plane directions. Thus, composites can be made lighter and thinner than conventional isotropic materials. Another advantage of composites is that a laminate can be designed to satisfy a particular case, that is, the layup can be "formed" to get the strength and stiffness required in a specific application.

Composite shell structures have been widely used in aerospace applications. Wing skins and fuselage panels are some examples of these applications. They are also called thin-shell structures. The excessive vibration in these structures could cause fatigue failure or

shorten their useful life, and thus dynamic analysis becomes important in order to prevent collapse of these thin-shell structures. Since the strength varies from ply to ply in a laminate, composite materials are complicated to analyze, therefore numerical techniques must be considered in order to solve these problems.

1.1 Background.

Much work has been done in the area of composite cylindrical shells over the last few years. It has long been known that Classical Plate Theory, based on the Kirchhoff-Love hypothesis, tends to produce large errors when dealing with composite materials. The Kirchhoff-Love hypothesis assumes that straight lines normal to the undeformed shell midsurface remain straight and normal. In other words, transverse shear strains are neglected, resulting in overestimates of the natural frequencies.

Reissner was the first to recognize the need to include the effects of transverse shear effects; Mindlin followed, and added the effects of rotatory inertia. The so called Reissner-Mindlin theory assumes that while cross sections remain plane, they are allowed to rotate. This theory, however, does not satisfy the boundary conditions of zero transverse shear on the top and bottom surfaces of the shell. That requires application of a correction factor, and is commonly accepted.

Reddy [13,14] assumed that the displacements of the midsurfaces are cubic functions of z. This leads to a parabolic distribution for the transverse shear strain, and does not require

a correction factor. Linneman and Palazotto [12] used this approach in developing solutions for the natural frequencies for symmetric cylindrical composite shells. The dynamic response of cylindrical composite panels has been investigated, here at AFIT, in previous studies. Walley [24] studied the dynamic response of a curved Graphite/Epoxy (Gr/Ep) panel clamped all around with centered cutouts (2" x 2", 2" x 4", 4" x 4"). Cyr [4], using the same panels, studied the effect of cutout orientation on the natural frequencies and mode shapes of those panels. Levraea [7], using a finite element code called STAGSC-1, investigated the eccentricity effects of square cutouts on the natural frequencies and mode shapes of curved composite panels. And Silva [16] investigated a composite cylindrical shell panel under transverse load with through the thickness and snapping. Tsai and Palazotto [22] investigated the non-linear vibration of cylindrical shells with high-order shear deformation theory.

1.2 Objectives.

Using certain panel geometries, this study will investigate the thickness effects on the natural frequencies and mode shapes for different boundary conditions and different ply orientation.

There were two different size panels considered in this study, the first one used for comparison had an arclength, height and radius of curvature of 0.305 m (12 inches), 0.2794 m (11 inches) and 0.305 m (12 inches) respectively. One ply lay up was analyzed, $[0^o/-45^o/+45^o/90^o]_s$ in which each ply had a thickness of 0.000127 m (0.005 inches),

giving a total of 0.002032 m (0.08 inches) in panel thickness. The second panel had an arclength, height and radius of curvature of 0.508 m (20 inches); two ply orientations were analyzed, $[0^{o}/90^{o}]_{s}$ and $[-45^{o}/+45^{o}]_{s}$. Each ply was 0.00635 m (0.25 inches) thick, giving a total panel thickness of 0.0254 m (1 inch).In order to facilitate ply notation, the panels mentioned will be called Panel 1, Panel 2a and Panel 2b respectively.

The boundary conditions considered for both panels were Simply Supported along the vertical edges and free along the horizontal edges (SFSF), and Simply Supported all Around (SS). The DSHELL finite element code was used to predict the first four natural frequencies. The dynamic capability of this program, in predicting the natural frequencies and mode shapes, was evaluated by comparing to a reference using the Galerkin technique.

1.3 Analytical Approach.

The numerical analysis was conducted using the DSHELL computer code. Previous analyses have been successfully conducted at AFIT using this finite element program but never a dynamic frequency response of cylindrical composite shells.

DSHELL assumes a parabolic shear strain which varies through the shell thickness and vanishes at the top and bottom surface. Although classical plate and shell theory for thin isotropic structures ignore shear stress through the thickness, it is not appropriate to do so with composite shells. The coupling of extensional, bending, and shear strain must be

taken into consideration.

DSHELL contains a built-in grid generator which was used to generate all of the finite element meshes required for this investigation. This program was selected for use in this study to continue verification of its dynamic capabilities.

II. Theory

Most aerospace structures are considered continuous systems and have distributed material properties. An aircraft wing can be considered as a beam with nonuniform mass per unit length and flexural stiffness while a fuselage panel can be treated as a cylindrical shell. Problems concerning the vibration of shells are considerably more complicated than their counterparts for beams or plates. Primarily, this is caused by the effects of the curvature on the shell equations and thus on the dynamic behavior. For shells, membrane and flexural deformations are coupled, and any theory must consider these effects simultaneously.

2.1 Natural Frequencies of Shells

In the classical laminated shell theory, through the thickness shear deformation is neglected according to the Kirchhoff-Love hypotesis that plane cross sections remain plane before and after deformation. Mindlin introduced a theory that allowed the cross section remain plane but rotate from the normal with respect to the mid-surface after deformation. The assumption of no cross sectional warping introduces error, especially at the top and bottom surfaces, since the boundary condition of zero transverse shear is not matched.

Reddy [13] introduced a new theory in which the displacements of the mid-surface were cubic functios of z. This lead to a parabolic transverse shear distribution wherein the

strains are maximum at the shell mid-surface and are zero at the top and bottom surfaces, satisfying the required thickness boundary condition. Fig 2-1, shows the transverse shear conceptsdisscussed above.

BEFORE DEFORMATION

Plane Cross Section

AFTER DEFORMATION

Kirchhoff Theory

Mindlin Theory
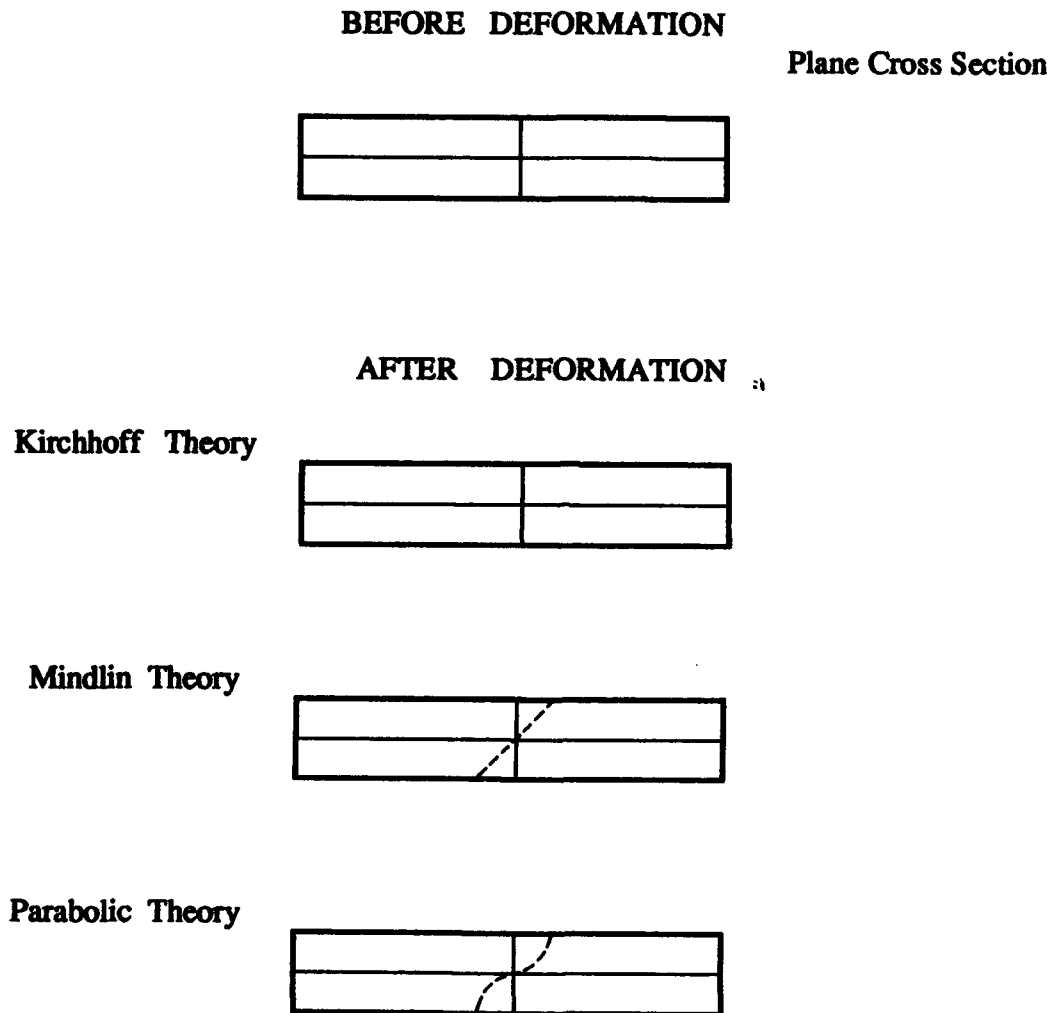
Parabolic Theory

Fig. 2.1 Transverse Shear Strain Theories

To achieve the desired parabolic shear distribution, a higher order displacement field is

required. This theory has been studied by Reddy [13] and also by Palazotto and Dennis [11]; both have presented higher order shear theories incorporating transverse shear effects, and this is certainly the most important feature of DSHELL. Tsai and Palazotto [22] incorporated the capability to performed dynamic analysis into this approach.

A description of the main features involved in DSHELL will be explained in order to clarify the theory behind this finite element program.

2.2 The K and M matrixes

This section is directed to the development of the appropriate vibration equations. The governing equation for the dynamic behavior of a continuous system, derived from the Hamilton's principle is [10:44]

$$m \ddot{X}(t) + c \dot{X}(t) + k X(t) = F(t) \tag{2.1}$$

where
m = system mass

c = system damping

k = system stiffness

t = time

$X(t)$ = displacement

$\dot{X}(t)$ = velocity

$\ddot{X}(t)$ = acceleration

F(t) = external forcing function

For free vibration there are no applied forces and therefore F (t) = 0. Structural damping is based on the energy losses caused by internal friction as the panel deforms and is proportional to the amplitude of displacement [10:402]. The extremelly small

2-3

displacements that take place in these cases, compared with the large stiffness of the system [21], justified neglect ng the damping effects, therefore c = 0. Thus, equation (2.1) becomes

$$m \; \ddot{X}(t) \; + \; k \; X(t) \; = \; 0 \qquad \text{continuous system} \qquad (2.2)$$

The [K] matrix, for an element modeling a composite material panel considering large displacements, is given by [22]

$$K(u) \; = \; Ko \; + \; \frac{K_1(u)}{2} \; + \; \frac{K_2(u)}{3} \qquad (2.3)$$

where Ko is a constant stiffness matrix, K_1 is a stiffness matrix related to linear displacement, and K_2 is a stiffness matrix related to quadratic displacement. For this analysis, the Ko matrix will be the only component used. The consistent mass matrix is obtained from [22]

$$M \; = \; \int_\Omega \sum_{k=1}^{L} \int_{\zeta_{k-1}}^{\zeta} \rho^{(k)} \; [N]^T \; [R]^T \; [R] \; [N] \; d\zeta \, d\Omega \qquad (2.4)$$

where ζ_{k-1} and ζ_k are positions at the top and bottom of the k th layer, Ω is the domain of the mid surface and L denotes the number of layers in the laminate. [R] is a matrix that is a function of ζ only. A full discussion this matrix is referred to reference [22], where

$[N]$ is the shape function matrix and ρ is mass per unit volume (density). The consistent mass formulation results in a fully populated, positive definite mass matrix.

The finite elment method requires the discretization of a continuous system into small elements in which the deformed geometry is represented by displacements at selected locations (nodes) within the body. Equation (2.2) can be written as

$$[M] \, \{\ddot{d}\} \; + \; [K] \, \{d\} \; = \; 0 \qquad \text{discrete system} \qquad (2.5)$$

where

$[M] = $ mass matrix $\qquad\qquad \{d\} = $ nodal displacement vector

$[K] = $ stiffness matrix $\qquad\qquad \{\ddot{d}\} = $ nodal acceleration vector

For harmonic vibration it is assumed that all nodal DOF are in phase and that $\{d\}$ in Equation 2.5 is given by [3:308]

$$\{d\} \; = \; \{d_0\} \, e^{i\omega t} \qquad\qquad (2.6)$$

where d_0 is the displacement amplitude, ω is circular natural frequency, and t is time. Substituting Equation 2.6 into Equation 2.5 gives

$$[K] \, \{d_0\} \; - \; \omega^2 \, [M] \, \{d_0\} \; = \; 0 \qquad\qquad (2.7)$$

Rearranging and changing notation, one obtains

$$[K - \lambda_i M] \{\phi_i\} = 0 \qquad (2.8)$$

where $\lambda_i = \omega_i^2$ ((rad/sec)^2) and the brackets have been dropped off of K and M for convenience (K and M are still matrices). For linear vibration analysis, K and M are independent of displacement and frequency. λ_i is the eigenvalue and $\{\phi_i\}$ is the eigenvector (mode shape) for the ith mode. Each eigenvector will represent a unique shape but with arbitrary amplitude.

Equation 2.8 represents the generalized eigenvalue problem for linear free undamped vibration [1:517]. If K and M are (n x n) matrices, then the solution to Equation 2.8 yields λ_i and $\{\phi_i\}$ for i = 1, 2, 3, ...n. The eigenvectors are independent and thus form a basis for the eigenspace [1:49]. The eigenvectors can be arranged into a (n x n) modal matrix given by

$$\Phi = [\{\phi_1\} \{\phi_2\} \ldots \{\phi_n\}] \qquad (2.9)$$

where the columns of the modal matrix are the eigenvectors of the system. This allows Equation 2.8 to be written as [1:558]

$$K\Phi = M\Phi\Lambda \qquad (2.10)$$

Here, Λ is a diagonal matrix of the eigenvalues, λ_{ii} and their location along the diagonal is determined by $\lambda_{11} < \lambda_{22} < \ldots < \lambda_{nn}$. The location of $\{\phi_i\}$ within Φ must be consistent

with the location of λ_{ii} in Λ; that is, $\{\phi_i\}$ is the corresponding vector for λ_{11}.

To solve the eigenvalue problems DSHELL uses a subspace iteration scheme. The procedure implemented in DSHELL is based on the subspace iteration method developed by Bathe [1:672-682].

2.3 Subspace Iteration Method.

The purpose of this section is to discuss the subspace method incorporated in the DSHELL code to find the eigenvalue-eigenvector. Appendix A indicates some additional details.

The basic objective in the subspace iteration method is to solve for the lowest p eigenvalues and corresponding eigenvectors satisfying [1:672]

$$K\Phi = M\Phi\Lambda \qquad (2.11)$$

where $\Lambda = \text{diag} (\Lambda_i)$ and $\Phi = [\phi_1, \phi_2, ..., \phi_p]$

In addition to Equation (2.11), the eigenvectors also satisfy the orthogonality conditions

$$\Phi^T K\Phi = \Lambda; \qquad \Phi^T M\Phi = I \qquad (2.12)$$

where I is an unit matrix of order q because Φ stores only q eigenvectors. The first

relation is a necessary and sufficient condition for the vectors in Φ to be eigenvectors, but the eigenvector orthogonality conditions in the second expression are necessary but not sufficient.

The number of modes desired are "p" , by using subspace iteration the reduced number of "p" eigenvectors are simultaneously obtained. The procedure modifies Bathe's subspace method in order to enhance convergence.

Subspace iteration reduces an ($n \times n$) eigensystem into a ($n \times q$) system where "q" is as defined before. The subspace refers to the space spanned by the reduced set of eigenvectors space [1:675]. If the subspace which is spanned by the reduced eigenvectors is denoted E_q , then the starting iteration vector can be thought of as spanning the E_1 subspace. As iterations are performed, the E_k (k=1, 2, 3,..., q) space approaches the E_q space. The E_q space is in effect spanned when the desired accuracy has been obtained.

The following gives an outline of the eigensolution technique used by DSHELL. First, a preliminary set of independent vectors is chosen which spans a subspace of the complete set of eigenvectors determined by the actual number of vectors desired (i.e. $2p$ or $p + 8$ which ever is smaller). Next, an inverse power method (inverse iteration) with shifting is performed (the shifting is used to overcome any matrix singularities). This transforms the E_k space into E_{k+1} space. Now the projections of K and M are found on the new reduced eigenspace (subspace E_{k+1}) yielding $K_{k+1} K_{k+1}$ and M_{k+1} respectively [7]. The

reduced ($n \times q$) eigenvalue problem is solved using Householder's Method with a LR algorithm. Finally, a check for convergence of the eigenvalues is made and the process repeated until adequate convergence has been obtained. The criteria for determing convergence is based upon the "$k + 1$" iteration eigenvalues being compared to the "k" iteration eigenvalues. If the relative error is below a predetermined threshold then convergence is assumed.

2.4 Thickness and Curvature Parameters.

In considering a cylindrical shell, there are two geometric parameters by which a shell can be described. The ratios δ/c and δ/h are used to explain the deepness and thickness of the shell respectively in subsequent sections. The following figure shows a typical shell element in which these parameters are given.
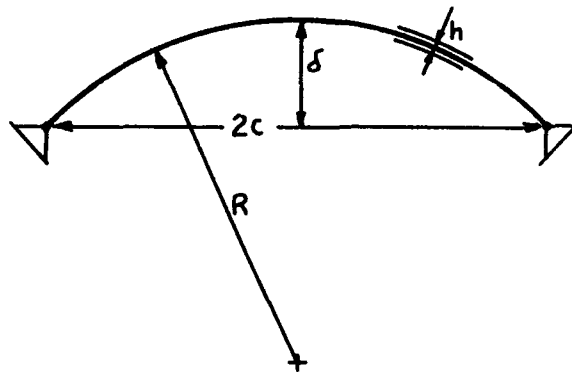
Fig 2.2 Typical Shell Element

From fig. 2.2, δ is the offset distance measured from the cord line to the datum surface of the shell, h is the thickness of the shell and c is half the distance of the cord.

2-9

The concept of deepness and shallowness is very useful when dealing with shells. A shell is considered shallow when the ratio δ/c is small, usually $\delta/c \leq 1/4$, [11:202]. A shell with $\delta/c \geq 1/4$ is considered deep. A deep shell has more coupling between displacements functions. The in-plane displacements u and v are affecting the rotation about a normal to the shell surface. DSHELL includes these effects, and thus it is possible to determine when they are of importance by studying eigenvector relations. In addition, a shell may be considered thick when the ratio $\delta/h < 1$ [11:203].

According to the objectives of this study, the effects of thickness and curvature on composite cylindrical panels will be evaluated, therefore the following figure, considering the case of the $[0^\circ/90^\circ]_s$ ply orientation, with $b/h = 20$ under the simply supported all around boundary condition (discussed in Chapter IV), will help to visualize when a shell is considered thick and or deep.
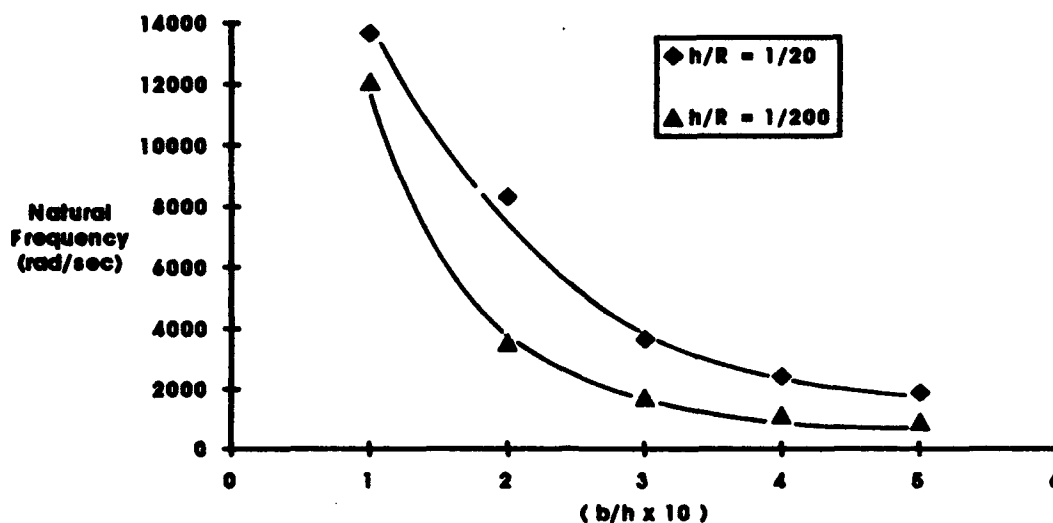
Fig 2-3 Typical behavior of the Fundamental Frequency for the $[0^{o}/90^{o}]_{s}$ ply orientation, Simply Supported all around Boundary Condition.

The following table shows the values for δ/c and δ/h ratios for the interval b/h and the curvatures showed in the figure above. The geometry of the shell and the parameters δ/c and δ/h involved are given in figure 2-2.

R = 20	θ = s/R	δ = R(1-cosθ/2)	c	δ/c	δ/h
b/h = 10	28.64^{o}	0.62	4.95	0.125	0.621
b/h = 20	57.29^{o}	2.45	9.58	0.254	2.44
b/h = 30	85.94^{o}	5.36	13.62	0.393	5.36
b/h = 40	114.59^{o}	9.19	16.83	0.546	9.19
b/h = 50	143.24^{o}	13.70	18.97	0.722	13.70
R = 200	θ = s/R	δ = R(1-cosθ/2)	c	δ/c	δ/h
b/h = 10	2.86^{o}	0.062	4.97	0.0125	0.062
b/h = 20	5.73^{o}	0.249	9.97	0.0252	0.249
b/h = 30	8.59^{o}	0.562	14.98	0.0375	0.562
b/h = 40	11.46^{o}	0.999	19.96	0.050	0.999
b/h = 50	14.32^{o}	1.427	23.84	0.0598	1.427

Table 2-1. Geometric Parameters of the Composite Shells

According to this table, for a radius R = 20, a shell with a span equal to ten (b/h = 10) is shallow (δ/c = 0.125), but also, at the same time, this shell can be considered thick since δ/h = 0.62. As the span increases, the shell becomes deeper since δ/c is greater than 0.25 but also it becomes thinner. For a radius of curvature R = 200, no matter what the span b, the shell is called shallow. It can be considered thin only for values b/h ≥ 40.

The curvature also has importance in the behavior of the frequency response for the case of cylindrical shell panels. According to fig. 2-3, as the radius of curvature decreases to h/R = 1/20, the frequency increases. This behavior is due to the fact that the in-plane displacements, u and v, have more effect on the natural frequencies when the panel becomes deeper (when the radius of curvature decreases). Then for the ratio h/R = 1/200, these effects are practically negligible. In order to understand this statement, the next figures show the magnitude of the in-plane displacements for the case of the [-45°/+45°]$_S$ laminate, simply supported-free boundary condition and b/h = 20 for two radius of curvature: 1/20 and 1/200.
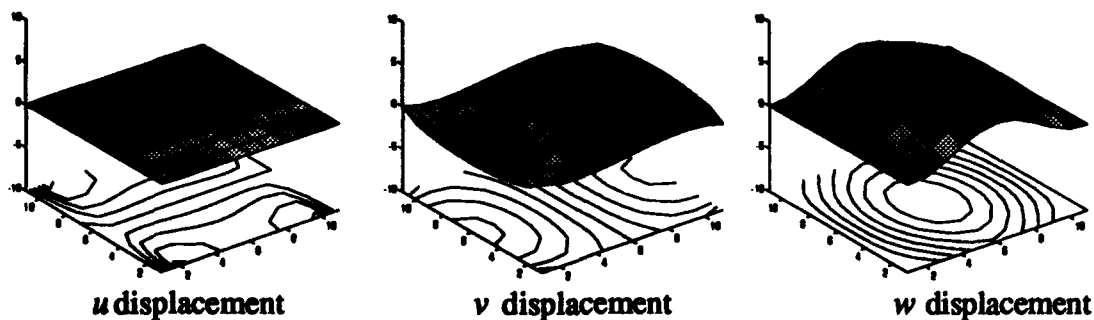
u displacement   v displacement   w displacement

Fig. 2-4   In-Plane Displacements for the [0°/90°]$_S$ laminate, Simply
Supported-Free Boundary Condition, b/h = 20, h/R = 1/20.

| u displacement | v displacement | w displacement |
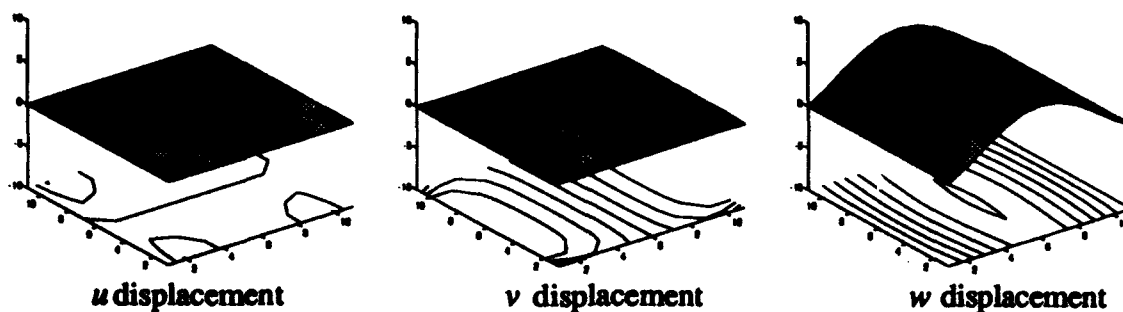
Fig. 2-5 In-Plane Displacements for the $[0^{\circ}/90^{\circ}]_S$ laminate, Simply Supported-Free Boundary Condition, b/h = 20, h/R = 1/200.

From the output of DSHELL, it was found that for h/R = 1/20, $u_{max} = 0.0522\ w_{max}$

and $v_{max} = 0.246\ w_{max}$, while for the ratio h/R = 1/200, $u_{max} = 0.00522\ w_{max}$ and

$v_{max} = 0.0245\ w_{max}$. It means that the in-plane displacements contribute ten times more

to the overall eigenvector-eigenvalue solution for the h/R = 1/20 than the ratio h/R =

1/200. It should be noted that the DSHELL program is always developing eigenvectors

and eigenvalues in which all the degrees of freedom are considered, as oppose to analyses

in which in-plane displacement and rotatory inertias are suppressed. Thus, by looking at

the maximun ordinate of the respectivedisplacements functions, one can obtain an

appreciation of the overall contribution to the global eigenvector. The same thing was

also observed for the rotation contribution Ψ_1 and Ψ_2.

2-13

III. Finite Element Analysis and Modelling

3.1 Panel Properties, Geometry and Assumptions.

The material properties and geometry of the panels are explained in this section. The analyzed panels are made of graphite/epoxy (Gr/Ep) material, they are cylindrical in shape and have different ply orientation. For consistency with previous works [7,8] a quasi-isotropic $[0^o/-45^o/+45^o/90^o]_S$, $[0^o/90^o]_S$, and $[-45^o/+45^o]_S$ ply layup were selected. They will be referred as Panel 1, Panel 2a and Panel 2b respectively. Table 3-1 lists the material properties for the panels referred above; the properties for Panel # 1 were obtained from experimentation [7] while the properties for Panel # 2 were taken as they were assumed using the Galerkin technique.

Mechanical Properties	Panel # 1	Panel # 2 (a and b)
E_1 [GPa]	141.06	144.79
E_2 [GPa]	9.238	9.652
G_{12} [GPa]	5.955	4.136
G_{13} [GPa]	5.955	4.136
G_{23} [GPa]	2.977	2.068
ν_{12}	0.3131	0.300
ν_{21}	0.0205	0.020
ρ [Kg/m^3]	1612.02	1522.3

Table 3.1   Material properties of Composite Panels

In Panel 1 each ply was 1.27×10^{-4} m thick resulting in a panel thickness of 0.002 m. Panels 2a and 2b had a ply thickness of 0.00635 m, resulting in a panel thickness of 0.0254 m.

The curvilinear orthogonal coordinate system and nomenclature used in this formulation of the laminated cylindrical shell is shown in Fig. 3-1. The x-axis lies along the straight dimension of the panel; the s-axis follows the circumference, and the z-axis is everywhere normal to the shell middle surface, positive toward the center of curvature. The surface formed by the x and s axes lies in the center of the thickness of the panel, so the thickness coordinate is negative on the outer surface and positive on the inner surface. Displacements along the x, s and z axes are u, v and w respectively. The angle ϕ specifies the orientation angle of each ply in the laminate. The effective panel dimensions are defined as the dimensions of that portion of the panel free to vibrate.
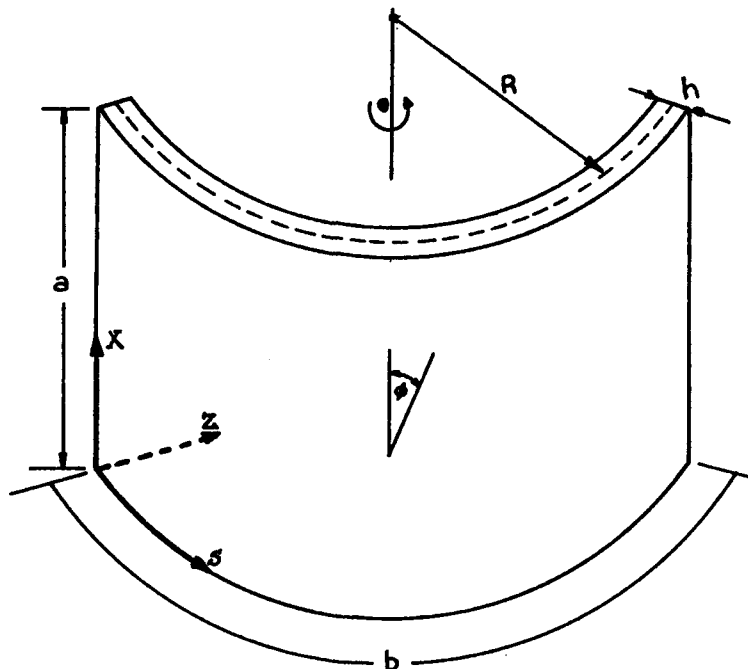
Fig 3-1. Shell Panel Dimensions and Coordinate System

Two boundary conditions were analyzed for both panels: Simple Supported-Free (SFSF; circumferential edges are free) and Simply Supported all around (SS). The panel characteristics cited in this section were used to create part of the finite element models (input data).

3.2 DSHELL Program

According with the finite element analysis, the modelling of cylindrical shells have been done through the following theories:

a) Flat Elements: Plane bending elements with plane membrane elements

b) Curved Elements: Classical shell theory

c) Mindlin type elements: special forms of solid elements

The DSHELL finite element program, used in the present study, uses the type of elements described in part (c). This finite element code was originally written by S. Dennis [11] and modified by C. T. Tsai and Palazotto [22]. The uniqueness of the DSHELL program is that shear strains are assumed to vary parabolically through the thickness of the shell, vanishing at the top and bottom surface, large displacements and rotations are considered.

DSHELL also incorporates material linearity. In structural applications, materials are normally restricted to the linear elastic region [6]. This implies that any fiber breakage during large displacements and rotations is ignored.

The majority of past efforts has dealt with static analysis or with the dynamic analysis but without taking account of the eigenvector problem. Therefore, this thesis will serve to further validate the dynamic modeling capabilities of the DSHELL program. A linear, free vibration analysis was conducted on the Gr/Ep circular cylindrical panels. For free vibration analysis, DSHELL outputs the desired natural frequencies and corresponding eigenvectors. They represent the mode shapes of the panel.

The user has the capability of selecting the type of element under study : plate or cylindrical shell, number of nodes per element and type of analysis: nonlinear, linear or eigenvalue problem. Also the number of natural frequencies required and type of laminate can be set. In addition, the built-in mesh generator was used to establish the finite element grid for all the panels.

The user can determine the number of elements in the x and y direction, the grid spacing in the same coordinate directions and DSHELL determines the nodal coordinates and connectivity matrix. Any of the degrees of freedom at each node can be restrained according to the boundary conditions desired. Finally, the material properties must be input: density, Young's modulis, shear modulus, Poisson's ratio, number of plies, ply orientation angles, ply thickness and circular cylinder radius. For the type of analysis performed and the panel geometries investigated, DSHELL proved a straight forward implementation.

3.3 Element Selection.

The DSHELL finite element program uses a 36 DOF element developed by Dennis [11] and pictured in Fig 3-2. The seven displacements functions $u, v, w, w_{,1}, w_{,2}, \Psi_1$ and Ψ_2 are considered in each element. The mid-side nodes have only the two inplane degrees of freedom u and v. Lagrangian bilinear interpolation is used for Ψ_1 and Ψ_2, quadratic interpolation is used for u and v, while non conforming Hermitian interpolation is used for w, $w_{,1}$ and $w_{,2}$. Although a shell is three dimensional, a two dimensional formulation is used to model a thin shell.
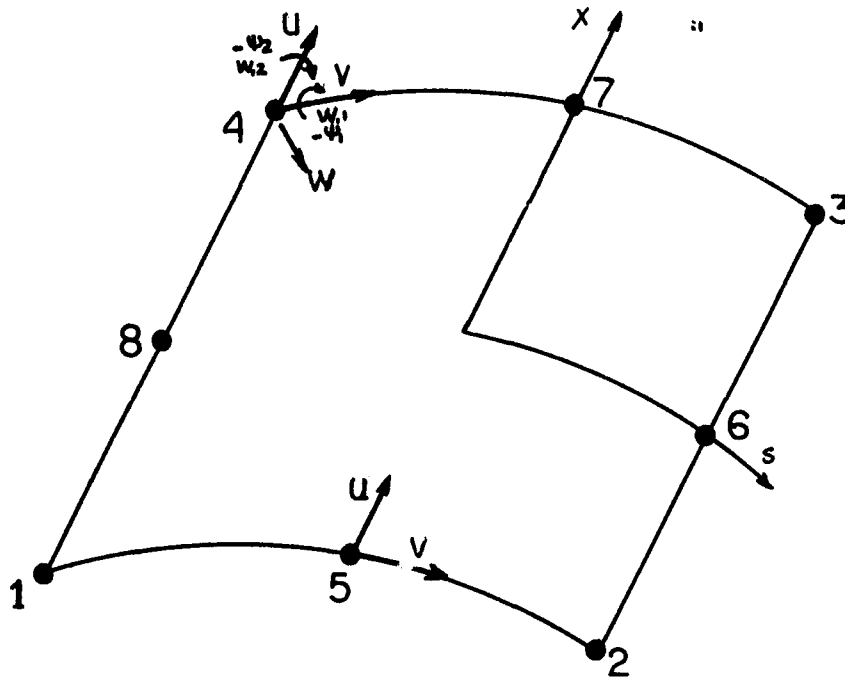
Fig 3-2. 36 DOF Isoparametric shell element

where : $\xi = x/a$ and $\eta = s/b$, the natural curvilinear coordinates of the surface

u is the displacement in the x coordinate direction

v is the displacement in the s coordinate direction

w is the transverse displacement in the z coordinate direction

$w_{,1}$ is the slope $\partial w / \partial x$ at the node

$w_{,2}$ is the slope $\partial w / \partial s$ at the node

Ψ_1 is the rotation of the normal to the shell midsurface in the x direction

(about the s axis)

Ψ_2 is the rotation of the normal to the shell midsurface in the s direction

(about the x axis)

The overall equation defining the isoparametric discretization of the continuum

displacements into discrete displacements is obtained by [19]

$$| u | \quad = \quad [N] \quad \{ q \}$$

$$(7 \times 1) \quad (7 \times 36)(36 \times 1)$$

3.4 Convergence Study.

A convergence study was carried out for the dynamic response of composite panels.

This study was conducted using the 36 DOF element described before and Panel # 1

(explained in section 3.1). This panel had been analyzed before [7], using the STAGSC-1 finite element code, and experimentally by Holographic Interferomerty. Since results from these methods were available, this panel, under its respective boundary condition, was chosen only to prove the precision of the DSHELL code in predicting the natural frequencies and mode shapes.

The DSHELL built-in grid generator was used to create all element meshes. This resulted in meshes composed of rectangular elements. The following pattern was used: the number of elements or nodal divisions in the s direction (according to fig. 3-1) was varied while the number of elements in the x axis kept constant. Then, when the number of elements in the s direction were kept constant, the number of elements in the x axis were varied.

Fig 3-3 shows the behavior of the frequencies when the number of divisions in the x axis were 10, 15 and 30 elements respectively. It is seen from these curves that, as the number of elements increase the difference between reference [7] and this analysis becomes smaller.

Fig 3-4 show the behavior of the frequencies when the divisions in the s direction were varied, the same intervals were analyzed and now the first two modes were affected when more than 15 divisions were used in that direction. The higher modes converged to the reference solution.
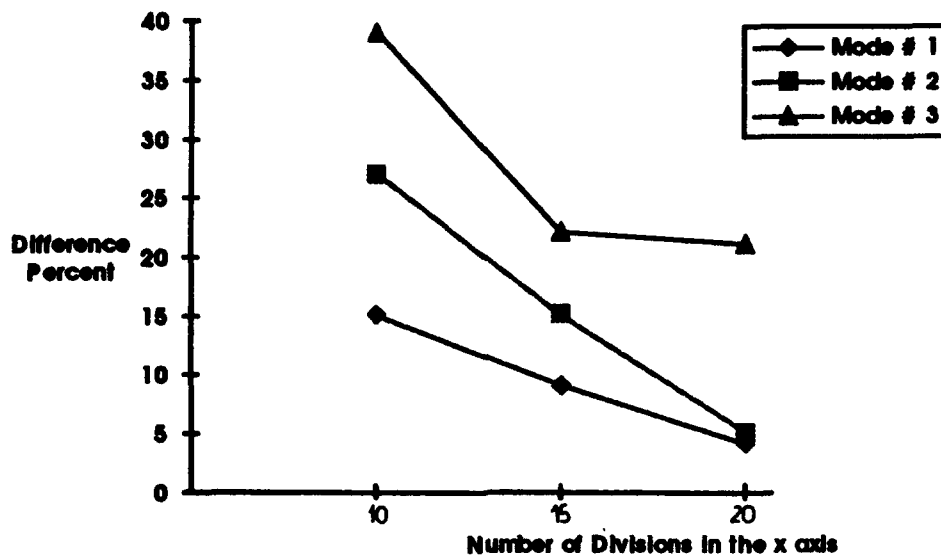
Fig 3-3   Percent Difference in the Frequencies by Varying the x Axis
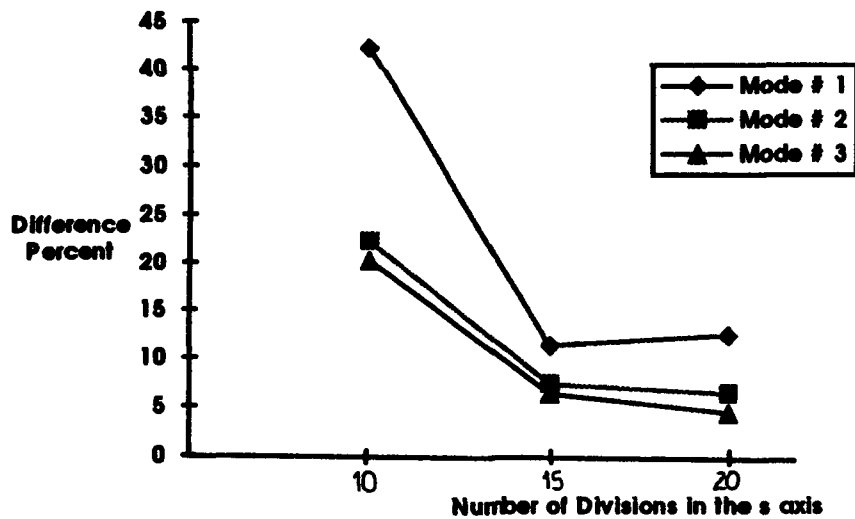
Fig 3-4   Percent Difference in the Frequencies by Varying the s axis

According to this analysis, ten divisions should be used in the x axis while fifteen elements were required in the s direction. When these results were combined in a mesh, the solution converged to the reference study and the average difference was about 4%.
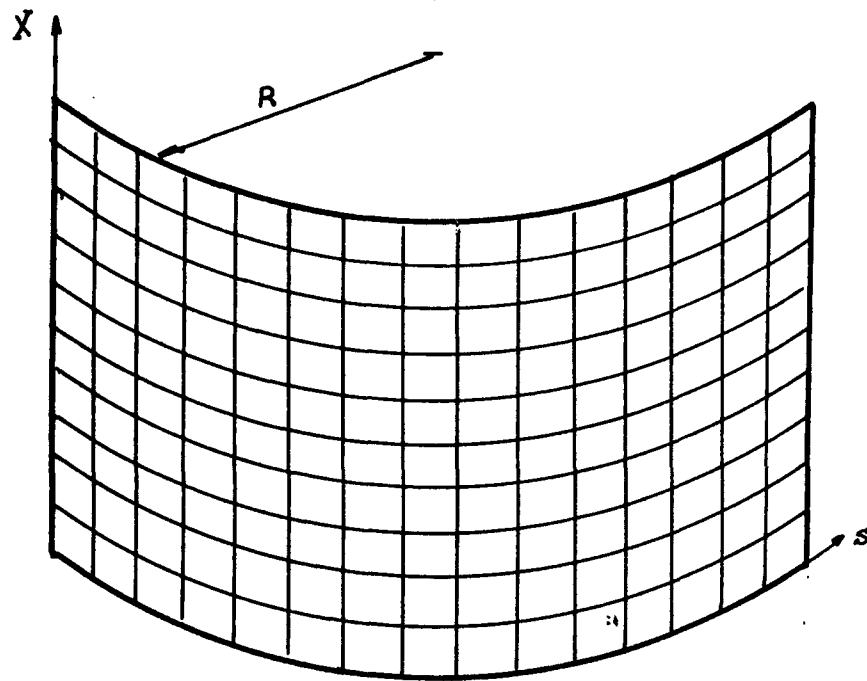
Fig. 3-5 Typical 10 x 15 Element Mesh

Some other mesh combinations were used and they are included in the next table.

Mode Number	Holographic Interferometry	Mesh 8 x 20	Mesh 10 x15	Mesh 11 x 12	Mesh 5 x 40
1	108.70	95.36	102.83	104.8	91.62
2	203.3	208.42	199.92	219.3	181.67
3	235.1	248.21	252.60	268.2	259.64
4	369.4	368.37	370.24	398.2	389.21

Table 3-2 Natural Frequencies (Hz) from Convergence Study for Panel # 1

Figures 3-6 and 3-7 show the mode shapes obtained for two meshes analyzed: the mesh used and the reference.
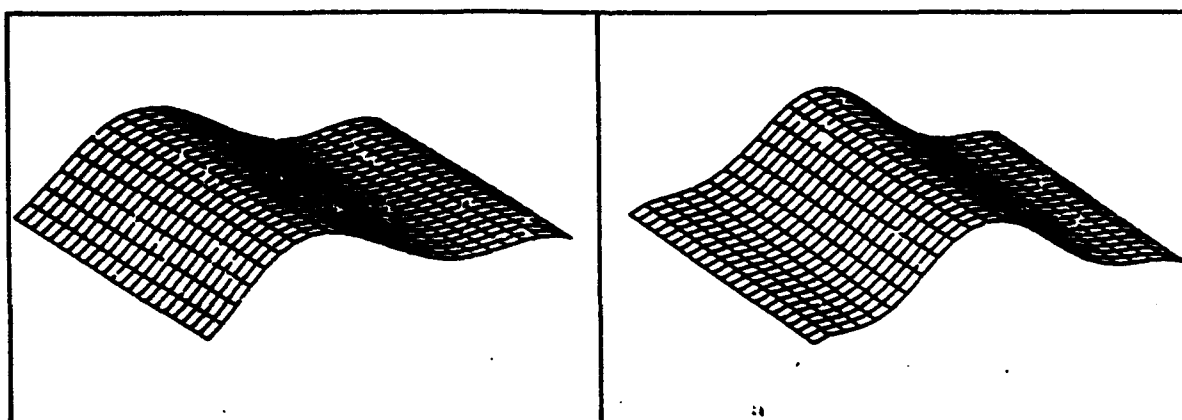
First Mode Shape   Second Mode Shape
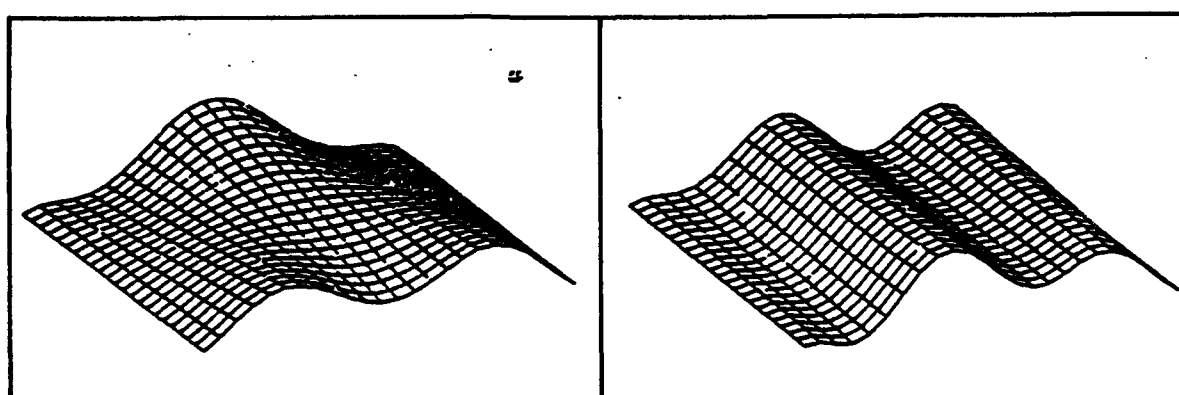
Third Mode Shape   Fourth Mode Shape

Fig 3-6. Mode Shapes for Panel # 1 according to the reference
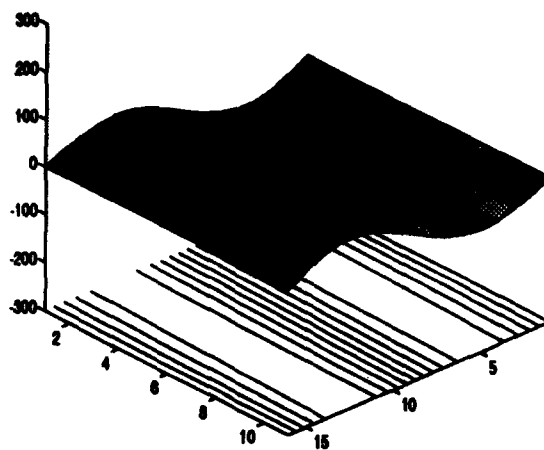
First Mode Shape
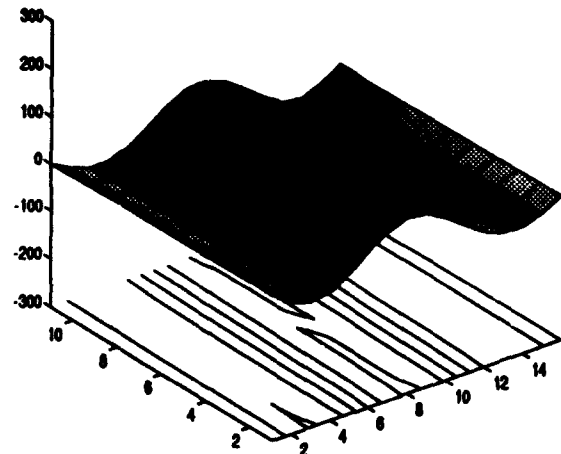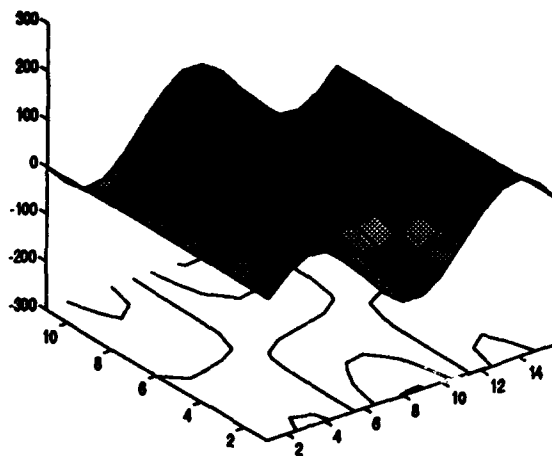
Second Mode Shape

Third Mode Shape
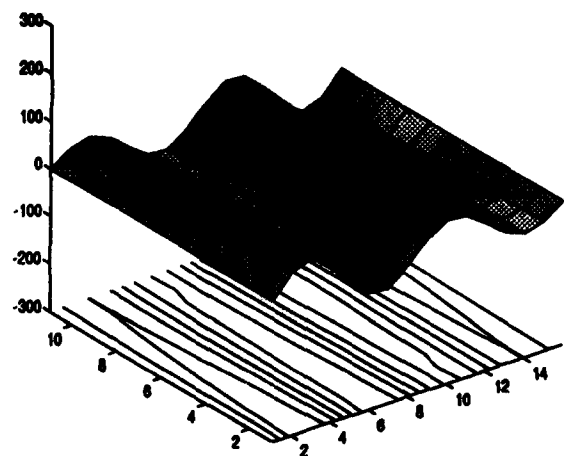
Fourth Mode Shape

Fig 3-7. Mode Shapes Panel # 1 using 10 x 15 Element Mesh

It was noticed also, from the convergence analysis, that it is necessary to have about four elements or divisions per each half-sine wave of modal displacement in order to obtain the precise mode shapes, this is also convenient for the eigenvalue solution.

It must be pointed out that there is an effect of the eigenvector space on the natural frequencies and mode shapes. In order to solve the eigenvalue-eigenvector problem, DSHELL uses, as it was explained before, the subspace iteration method. This algorithm, according to the number of eigenvalues requiered p, generates the number of starting iteration vectors q, where $q > p$ (actually $q = 2p$). DSHELL had been working with 10 starting iteration vectors, and it seems that they were not enough for solving the present problem, therefore and adjustment was made in order to obtain good results and actually the number of starting iteration vectors has been increased to fourteen and with that number, the solutions obtained were satisfactory. In order to show the change accuracy, the following eigenvectors using $q = 10$ and 14 are compared for a particular shell, as shown, considering the higher modes.

One will notice the improvement for $q = 14$, furthermore, a table comparison of the frequencies is also shown. It becomes apparent, that for certain cases a $q = 14$ vectors was satisfactory and thus this was used throughout.

(a) Using 10 vectors   (b) Using 14 vectors
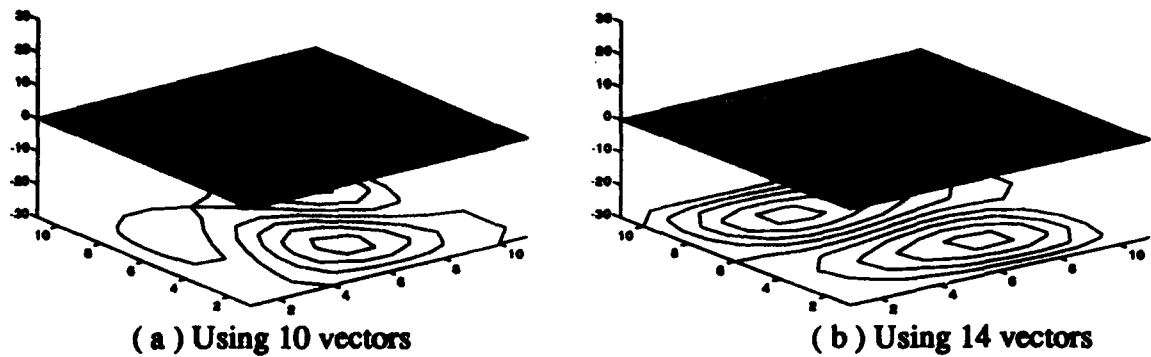
Fig 3-8. Third mode shape, $[0^o/90^o]_S$ ply orientation, Panel # 2,
All Edges Simply Supported Boundary Condition,
b/h = 20 and h/R = 1/20 using q = 10 and 14.

Also the following table shows the effects of increasing the number of vector iteration

from q = 10 to q = 14 on the third and fourth mode for the especified case.

	10	VECTORS	14	VECTORS
b/h = 10	Mode # 3	Mode # 4	Mode # 3	Mode # 4
h/R = 1/20	20398.18	20399.97	20461.18	20498.97
h/R = 1/50	20397.15	20398.14	20375.15	20419.14
h/R = 1/200	20395.14	21534.41	20309.14	20362.41
b/h = 15	Mode # 3	Mode # 4	Mode # 3	Mode # 4
h/R = 1/20	13598.94	13607.48	13598.58	13617.48
h/R = 1/50	13596.58	13598.38	13568.24	13586.38
h/R = 1/200	13500.43	13578.20	13500.43	13579.20
b/h = 20	Mode # 3	Mode # 4	Mode # 3	Mode # 4
h/R = 1/20	10205.80	10297.55	10208.94	10397.55
h/R = 1/50	9314.28	10269.94	9315.28	10269.99
h/R = 1/200	9088.64	10193.29	9089.63	10195.19

Table 3-3. Comparison between the Third and Fourth Natural Frequencies,
b/h = 10, 15 and 20, using q = 10 and q = 14 vectors.

IV. Results and Discussions

The primary objective of this thesis was to examine the thickness and curvature effects on the dynamic response (natural frequencies and mode shapes) of the circular cylindrical, Gr/Ep composite shells, using the DSHELL finite element program. Also the dynamic capabilities of this code will be evaluated by comparing to a reference using the Galerkin technique.

Previous analyses at AFIT concerning the dynamic response of solid cylindrical composite panels have been developed using the Galerkin technique and also including a higher order shear deformation theory (developed by Linneman & Palazotto in 1988).

A linear, free vibration analysis was performed on the panels described in Chapter III in which damping effects were assumed negligible and compared to experiments.

The mode shapes were created by plotting a surface-contour plot of the eigenvector output by DSHELL. To help visualize the mode shapes, orthographic views of the mode shapes are included.

The resulting analytical natural frequencies for this study and the ones obtained from the Galerkin technique are compared using a percent difference approach. In all cases, the percent difference for a given mode was calculated using the following relation

$$\text{Percent Difference} = \frac{f_{GALERKIN} - f_{DSHELL}}{f_{GALERKIN}} \times 100\%$$

where f_{DSHELL} is the finite element natural frequency using DSHELL and $f_{GALERKIN}$ is the natural frequency using the Galerkin technique. Both frequencies are given in Hertz (Hz).

Panel # 1:

This panel was selected as a baseline against which the model (using DSHELL) was compared. Since analytical and experimental results were available, the comparisons made helped us to obtained some important conclusions for further analyses.

The first consideration in analyzing the results was to look at the convergence of the eigenvalues and the respective eigenvectors. Different mesh configurations were studied: 8 x 20, 11 x 12, 10 x 15, but only one converged to the accepted result, the 10 x 15 element mesh configuration was chosen for modelling this panel.

Table 4-1 shows the predictions provided by DSHELL for the first four natural frequencies using the 36 DOF element and the 10 x 15 mesh configuration and the results from the reference study [7]. The effects of the degrees of fredom, especially at the corner nodes, on the mode shapes was also considered. Figure 4.1 shows a typical corner node element used in this analysis where the boundary conditions are specified.

Natural Frequency	Holographic Interferometry [7]	10 x 15 Mesh	Percent Difference
1	108,70	102,83	5.40 %
2	203,35	199,92	1.68 %
3	235,18	252,60	-7.40 %
4	349,42	370,24	-5.95 %

Table 4-1. Natural Frequencies (Hz) for Panel # 1
using the 10 x 15 mesh configuration
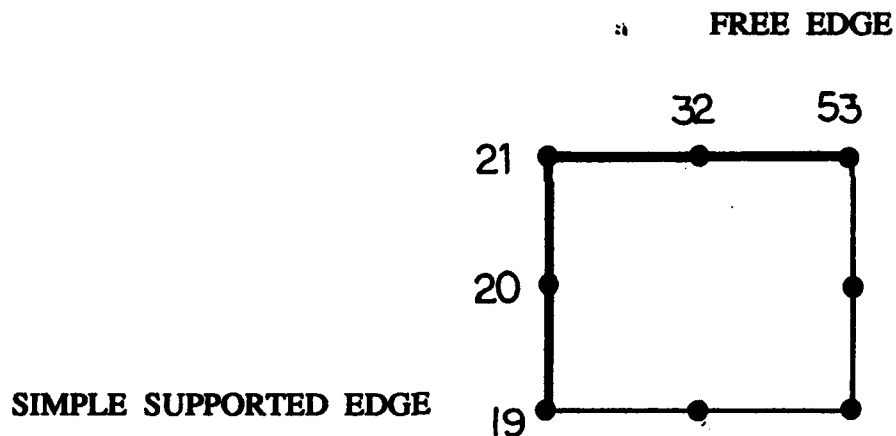
Fig. 4.1 Typical corner top element and respective node numbering
for the 10 x 15 element mesh

Two sets of degrees of freedom were analyzed at each corner node to see the effects of

physically varying the restraint to duplicate the actual test conditions.   Table 4-2 shows

the DOF used in the corner element specified above with both sets of DOF.   The

behavior of the mode shapes were not affected using these two approximations.

4-3

	NODE NUMBER	u	v	w	$w_{,1}$	$w_{,2}$	Ψ_1	Ψ_2
B.C. Option (a)	19	1	1	1	1	0	1	0
	20	1	1	0	0	0	0	0
	21	1	1	1	1	1	1	1
	53	0	0	0	0	0	0	0
B.C. Option (b)	19	1	1	1	1	0	1	0
	20	1	1	0	0	0	0	0
	21	1	1	1	1	0	1	0
	53	0	0	0	0	0	0	0

Where the number 1 stands for a restraint DOF
and 0 stands for a free DOF.

Table 4-2. DOF used at the corner nodes for Panel # 1

Frequency Number	Experimental Approach	Mesh 10 x 15 (a)	Mesh 10 x 15 (b)
1	108,70	102,83	78,50
2	203,35	199,92	176,07
3	235,18	252,60	209,80
4	349,42	370,24	338,05

Table 4-3. Effects of the DOF on the Natural Frequencies (Hz)
for options (a) and (b) shown in Table 4-2, Panel # 1

4-4
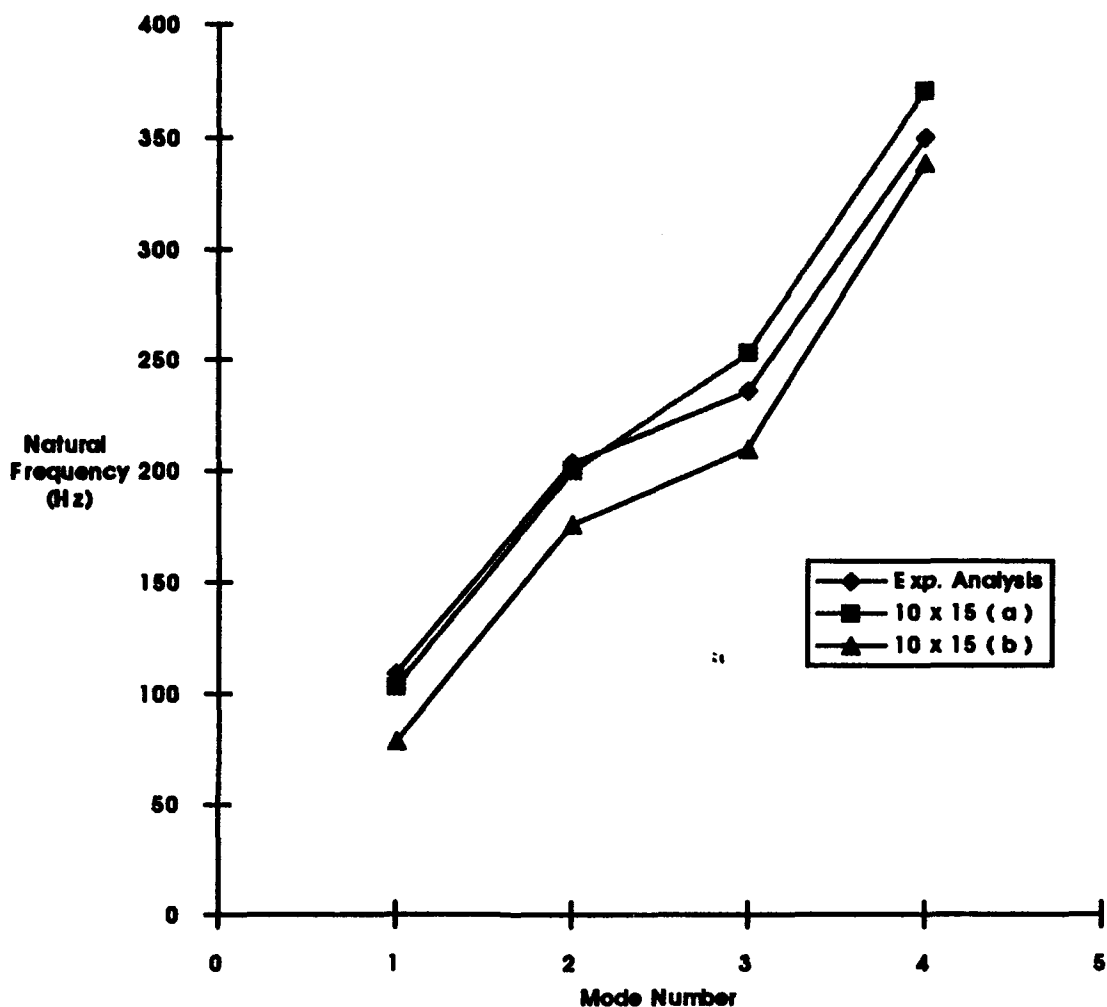
Fig. 4.2   Magnitude of the Natural Frequencies for the first four modes,
using Mesh element 10 x 15 (a), (b) and reference.

It was found that using the adequated degrees of freedom, option (a) specifically, the

panel converged in natural frequencies and mode shapes to the result obtained by using

STAGSC-1 code and the holographic experimentation [7]. Of course, absolute

convergence could not be proven. The largest percent difference was 7.40 % (above)

for the case of the third frequency, and the smallest was 1.68 % (below) for the second

natural frequency.   The first mode is followed by a substantial increase in frequency to a

relatively close second and third modes, followed by another substatial increase in

frequency for the fourth mode.

The mode shapes displayed the same behavior as the ones shown in the reference study.

A graphical representation of the mode shapes for this panel is given in Figure 4.3.   By

referring to this figure, it can be seen that the first mode was antisymmetric, the second

and third mode were symmetric, and the fourth mode again was antisymmetric. Therefore,
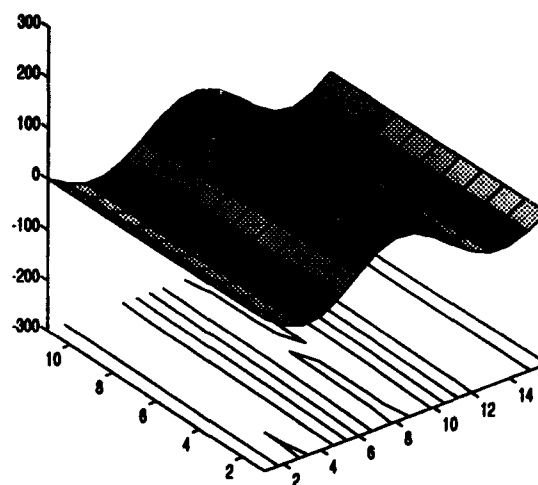
trasition from antisymmetric to symmetric modes and visa versa is accompanied by a large

increase in frequency, whereas adjacent modes which are closely spaced in frequency were

either both symmetric or both antisymmetric.
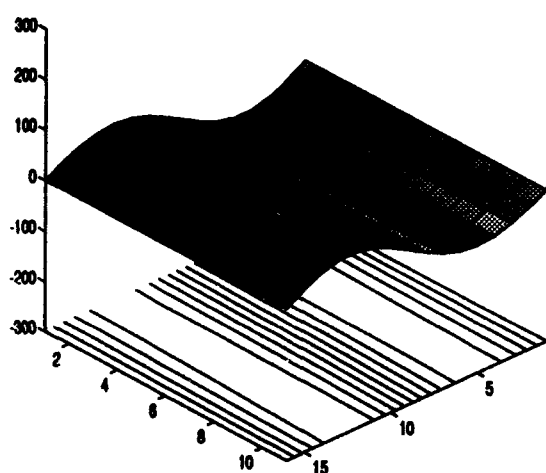
First Mode Shape   Second Mode Shape
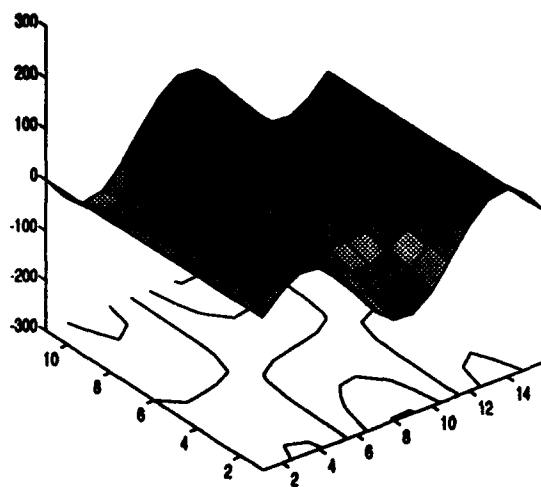
Third Mode Shape   Fourth Mode Shape

Fig. 4.3   Mode Shapes for Panel # 1, Simply Supported-Free
Boundary Condition.

It may also be observed that this panel is deep with $\delta/c =$ ⠀⠀and is thin since $\delta/h =$ ⠀⠀.

Therefore, it is expected that in-plane displacements enter the eigenvector as important

parameters while the through the thickness shear is unimportant.

Panel # 2:

Using the DSHELL code, this study investigated the thickness effects on the natural

frequency and mode shapes for a square panel varying the span to thickness ratio and the

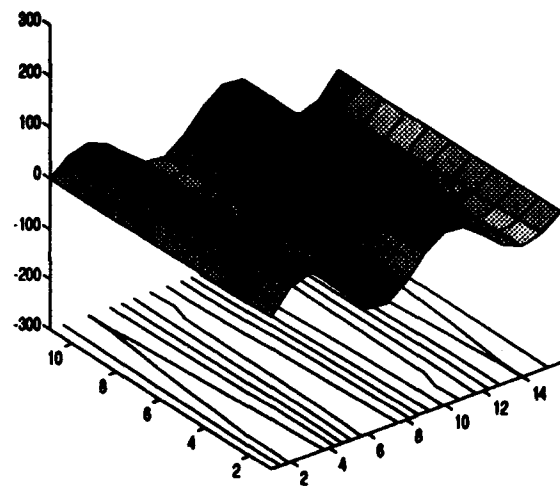curvature in order to measure effects on two ply orientations, $[0^o/90^o]_s$ and $[-45^o/+45^o]_s$

in which each ply was 0.25 inches thick, giving a total panel thickness of one inch.

Two boundaries conditions were applied: Simply Supported along the vertical edges and

free along the horizontal edges (SFSF) and Simply Supported all around (SS).

Different mesh configurations were also analyzed, but the 10 x 10 element mesh proved to

be the most adequate mesh for the present study.

NODE NUMBER	u	v	w	$w_{,1}$	$w_{,2}$	Ψ_1	Ψ_2
19	1	0	1	1	0	1	0
20	1	0	0	0	0	0	0
21	1	1	1	1	1	1	1
(32 *)	0	1	0	0	0	0	0
(53 *)	0	1	1	0	1	0	1

Table 4-4. Typical corner top element and the characteristic node numbering
for the 10 x 10 mesh configuration

Table 4-4 shows the DOF used in a typical corner element for this panel, and Figure 4.4 shows the specified element (corner top) above and the respective nodes numbering. The nodes with asteriks in that figure are only considered in the SS boundary condition.

FREE EDGE
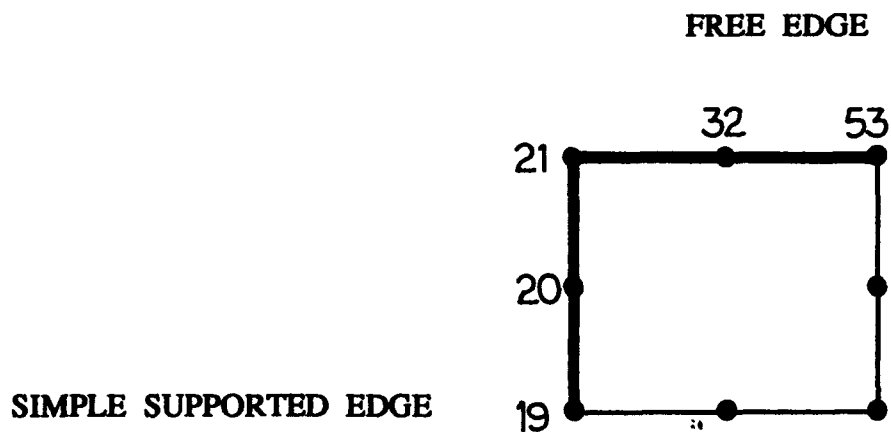
Fig. 4.4 Typical top corner element and the respective node numbering for the 10 x 10 mesh configuration

The panels studied were square, a = b = 1, where a and b are the edges along the x and s axis respectively; the thickness was assumed constant and for the boundary conditions specified, different ratios of thickness to radius of curvature, h/R, were assumed (1/20, 1/50 and 1/200) and specific values of circumferential length to thickness ratios, b/h (10, 20, 30, 40 and 50) were considered.

All Edges Simply Supported Boundary Condition.

Figure 4.5 shows the effect of curvature h/R on the natural frequencies for panel # 2,

$[0^o/90^o]_S$ ply orientation, with simply supported boundary condition.

Fig 4.5 Curvature Effects on the First Natural Frequency, Panel # 2,
Simply Supported Boundary Condition, $[0^o/90^o]_S$ laminate

Some important trends are identified; the natural frequencies are seen to increase as h/R

is increased (smaller radius of curvature). Also the effect of increasing the span to

thickness ratio, b/h, (making the panel deeper) is seen to lower the frequencies. In

addition, for relatively "close" Boundary Conditions (shallow panels), b/h = 10, a small

difference in the magnitude of the first frequency is shown for the three span to thickness

ratios studied; this behavior changes for relatively "further apart" boundaries, b/h > 40, where the large differences in frequency appeared. This implies that shallow panel response is insensitive to radius of curvature but as the panel becomes deeper the frequency is affected by the curvature.

Figure 4.6 shows the effects of the radius of curvature on the natural frequency for the $[-45^o/+45^o]_s$ laminate. The fundamental frequencies are seen to increase as h/R is increased but the frequencies decrease by increasing the span to thickness ratio.
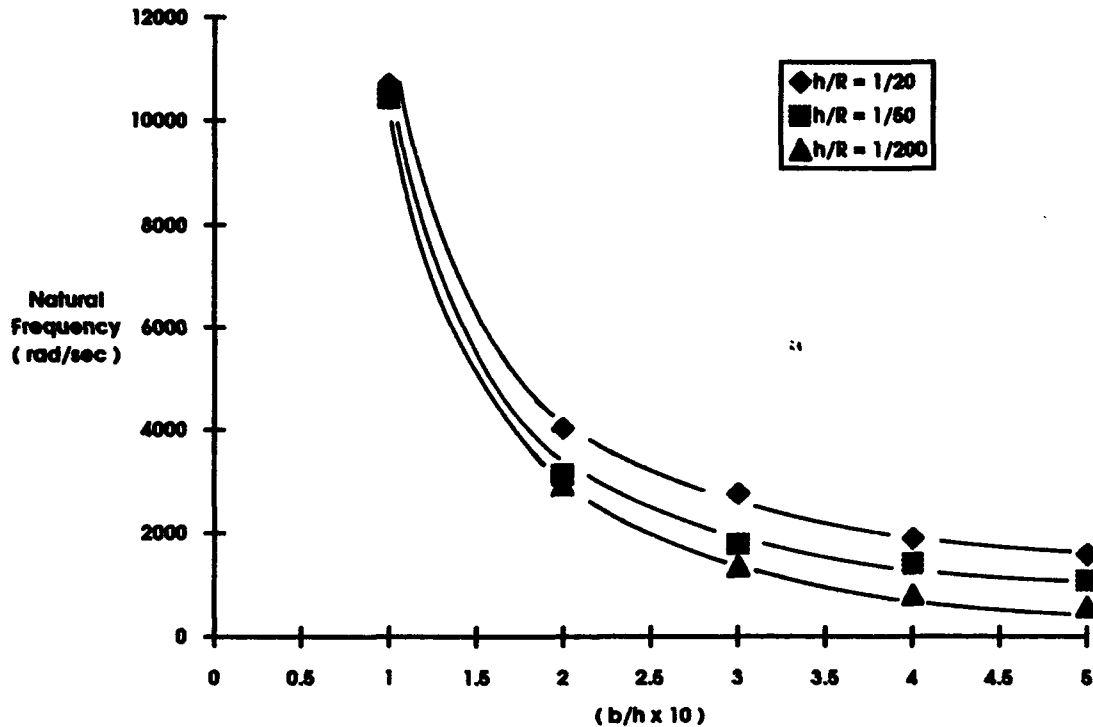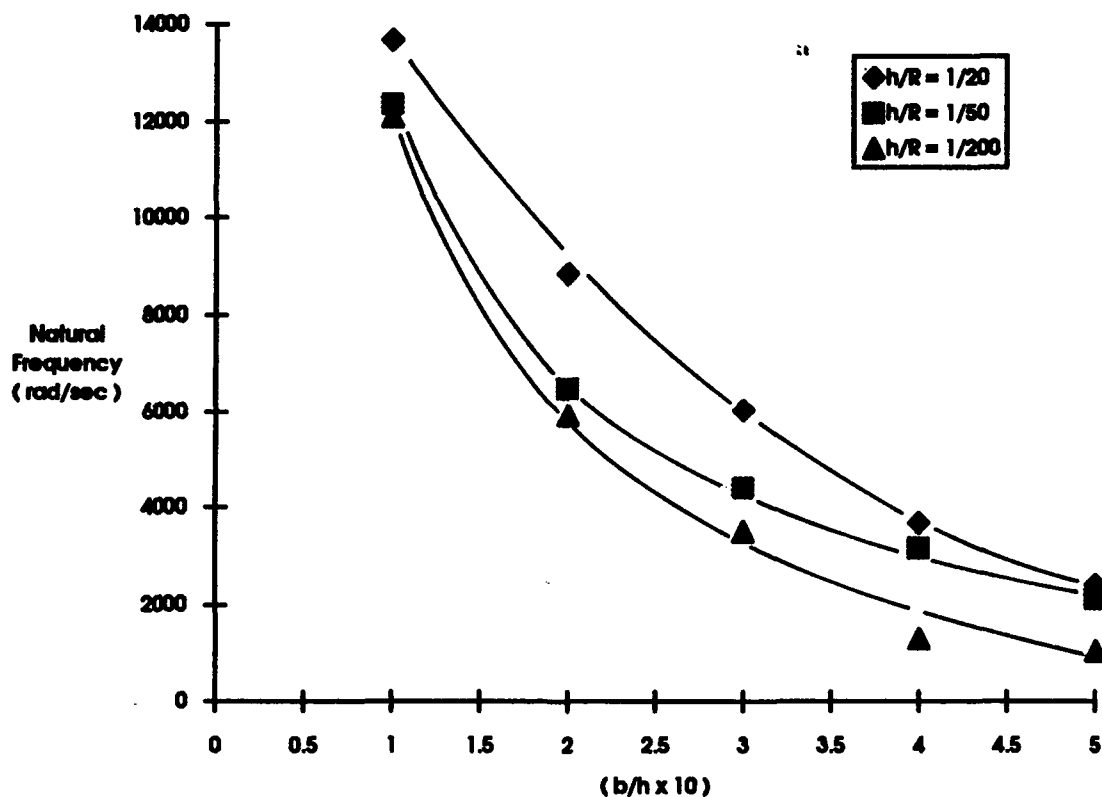

Fig 4.6   Curvature Effects on the First Natural Frequency, Panel # 2,
           Simply Supported Boundary Condition, $[-45^o/+ 45^o]_s$ laminate

The small difference in frequencies for "close" boundaries as seen in the last case, Fig 4.5, is present for the $[-45^o/+45^o]_s$ ply orientation for h/R > 1/50 (Fig 4.6). The larger h/R responded with the largest frequency no matter what shallowness parameter b/h was considered. From the figures above can be seen also that for shallow panels (δ/c very small), the δ/h implies thick panel and the effects of through the thickness shear is more noticed.

Comparisons can also be made between the natural frequencies obtained for the two laminates. Figure 4.7 shows the tendency of the curves for the fundamental frequency for the laminate orientations described, the value h/R = 20 was chosen for this analysis.
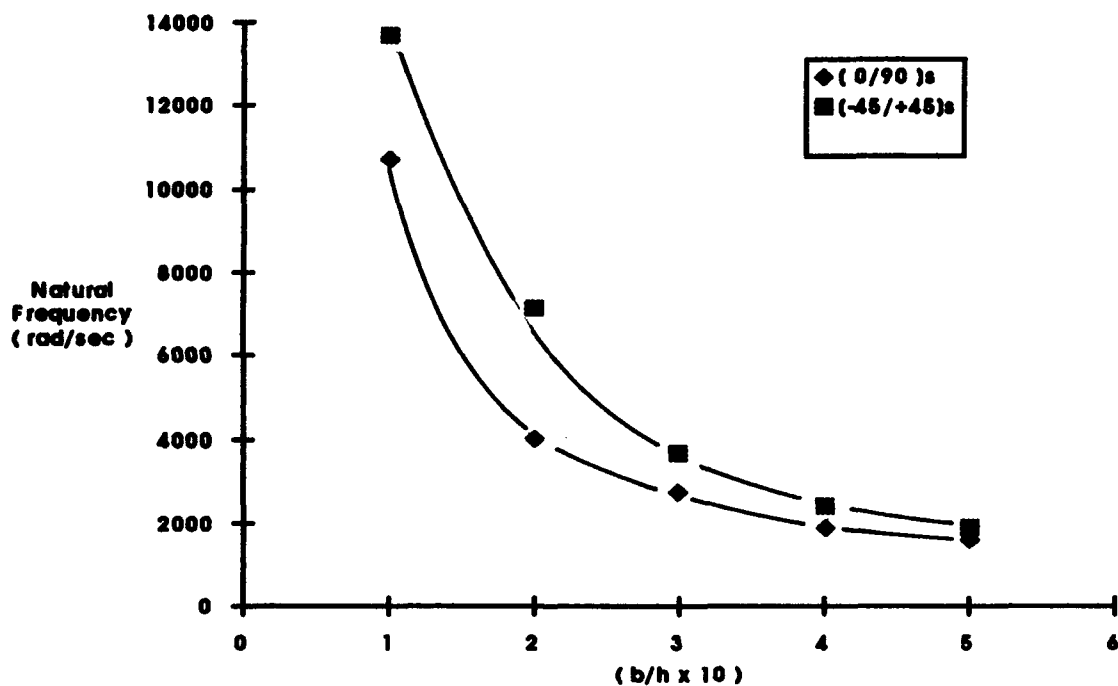

Fig. 4.7 Comparison for the Fundamental Frequency between the $[0^o/90^o]_s$ and
$[-45^o/+45^o]_s$ laminates, Simply Supported Boundary Conditionh/R = 1/20.

Both curves show the same behavior, the magnitude of the first frequency is higher for the $[-45^o/+45^o]_s$ than the $[0^o/90^o]_s$ laminate since that ply orientation makes the panel stiffer. This is because of the frequency equation depends on the extensional (A_{ij}) and bending coefficients (D_{ij}), [18:344], and they are higher for the $[-45^o/+45^o]_s$ than the $[0^o/90^o]_s$ laminate. Also, by increasing the span to thickness ratio, the first frequency decreases in both cases. In addition, for (b/h) < 30, the variation between the two frequencies is significant, but as b/h increases the comparison for the two lay-ups converge.

Up to this point these results are not new. Linneman [8] examined symmetrical laminates using two theories: Galerkin Technique and a Higher Order Shear Theory; the validation of the results in this analysis was obtained from comparison to his results.

The values for the first natural frequency using DSHELL and the Galerkin technique for the ratio h/R = 20 are shown below. The difference percent is also introduced. Table 4-5 shows the first natural frequency for this panel, $[0^o/90^o]_s$ laminate, with simply supported boundary condition. The highest difference obtained between the Galerkin technique and the DSHELL approximations was 11.34 % for the ratios b/h = 30 and h/R = 1/50.

Table 4-6 also shows the first natural frequency for the $[-45^o/+45^o]_s$ laminate, same boundary condition; the highest difference obtained between the Galerkin technique and the DSHELL approximations was 9.40 % for the ratios b/h = 50 and h/R = 1/20, while the lowest percent in difference was 1.08 %. The percent differences are relatively small, therefore DSHELL with the associated model was used for subsequent conditions.

b/h = 10	Galerkin Technique	DSHELL FEM code	Difference Percent
h/R = 1/20	10800	10702,7	+ 0,90 %
h/R = 1/50	10500	10482,2	+ 0,17 %
h/R = 1/200	N.A	10441,4	-

b/h = 20	Galerkin Technique	DSHELL FEM code	Difference Percent
h/R = 1/20	4200	4016,3	+ 4,36 %
h/R = 1/50	3200	3124,4	+ 2,36 %
h/R = 1/200	N.A	2919,2	-

b/h = 30	Galerkin Technique	DSHELL FEM code	Difference Percent
h/R = 1/20	2950	2760,3	+ 6,43 %
h/R = 1/50	2000	1773,2	+ 11,34 %
h/R = 1/200	N.A	1355,5	-

b/h = 40	Galerkin Technique	DSHELL FEM code	Difference Percent
h/R = 1/20	2000	1900,3	+ 4,98 %
h/R = 1/50	1450	1400,2	+ 3,43 %
h/R = 1/ 200	-	809,3	-

b/h = 50	Galerkin Technique	DSHELL FEM code	Difference Percent
h/R = 1/20	1700	1575,8	+ 7,30 %
h/R = 1/ 50	1100	1071,2	+ 2,62 %
h/R = 1/200	N.A	570,7	-

(N. A = Not Available)

Table 4-5 Comparison between DSHELL and the Galerkin Technique for the Fundamental Frequency, Panel # 2, $[0^o/90^o]_s$ ply orientation Simply Supported Boundary Condition.

b/h = 10	Galerkin Technique	DSHELL FEM code	Difference Percent
h/R = 1/20	14300	13672,2	+ 4,39 %
h/R = 1/50	12900	12349,6	+ 4,26 %
h/R = 1/200	-	12092,0	-

b/h = 20	Galerkin Technique	SHELL FEM code	Difference Percent
h/R = 1/20	7700	7285,9	+ 5,38 %
h/R = 1/50	4500	4389,5	+ 2,46 %
h/R = 1/200	N.A	3504,1	-

b/h = 30	Galerkin Technique	DSHELL FEM code	Difference Percent
h/R = 1/20	4000	3668,9	+ 8.28 %
h/R = 1/50	3200	3165,3	+ 1,08 %
h/R = 1/200	N.A	1720,8	-

b/h = 40	Galerkin Technique	DSHELL FEM code	Difference Percent
h/R = 1/20	2550	2414,9	+ 5,30 %
h/R = 1/50	2150	2107,7	+ 1,97 %
h/R = 1/ 200	N.A	1135,6	-

| b/h = 50	Galerkin Technique	DSHELL FEM code	Difference Percent
h/R = 1/20	2100	1902,7	+ 9,40 %
h/R = 1/ 50	1500	1463,6	+ 2,43 %
h/R = 1/200	N.A	906,1	-

(N.A = Not Available)

Table 4-6 Comparison between DSHELL and the Galerkin Technique
for the First Frequency, Panel # 2, $[-45^{o}/+45^{o}]_s$ ply orientation
Simply Supported Boundary Condition.

Although only the fundamental frequency has been included in the previous analysis, the eigenvectors corresponding to the first four natural frequencies for the $[0^O/90^O]_S$ and $[-45^O/+45^O]_S$ laminate, for b/h = 20, with Simply Supported all edges Boundary Condition are included in the next Figures. As stated in the modelling chapter, a subspace of 14 vectors was used throughout with a convergence tolerance on eigenvalues of 10^{-12}, thus twelve digit accuracy and six digit accuracy for the vector components of the eigenvector using a Rayleigh quotient relation [21]. The convergence equation is $\dfrac{\left| \lambda_i^{(k+1)} - \lambda_i^k \right|}{\lambda_i^{k+1}} \leq$ tol where k is the given iteration.
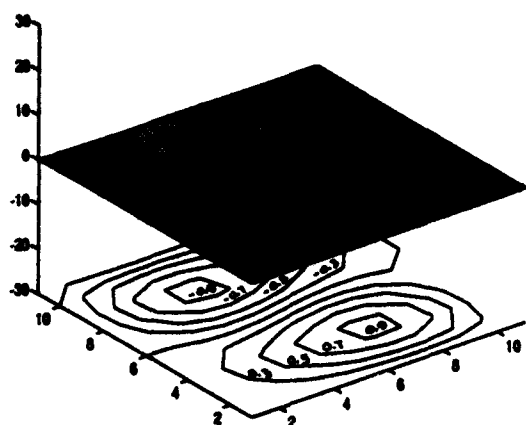
Fig 4.8 shows the mode shape for the $[0^O/90^O]_S$ laminate, under the simply supported all edges boundary condition, for the specific values of h/R= 1/20 and b/h = 20. The first mode is symmetric, the second, third and fourth mode are antisymmetric.
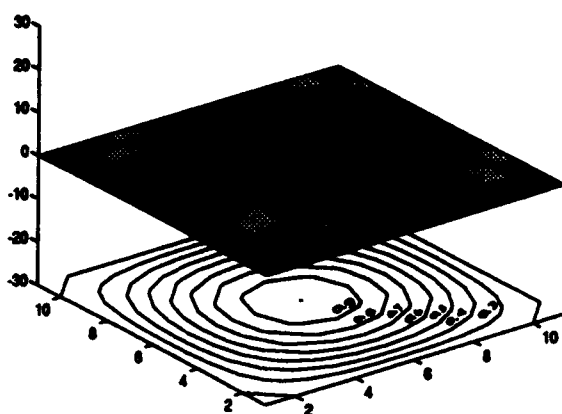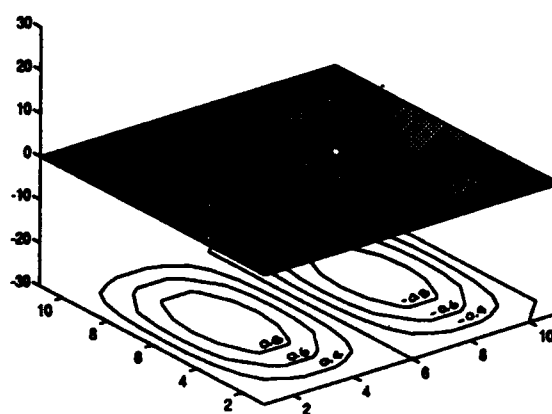
First Mode Shape   Second Mode Shape

Third Mode Shape   Fourth Mode Shape

Fig. 4.8   Mode Shapes for Panel # 2, Simply Supported Boundary
Condition, $[0^o/90^o]_S$ laminate, h/R = 1/20, b/h = 20

Fig 4.9 shows the mode shape for the $[-45^o/+45^o]_S$ laminate, under the simply supported

boundary condition, for the specific values of h/R= 1/20 and b/h = 20. The first mode is

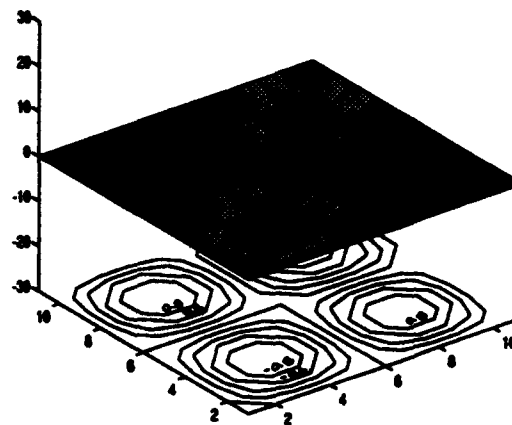symmetric; the second and third and fourth mode are antisymmetric.
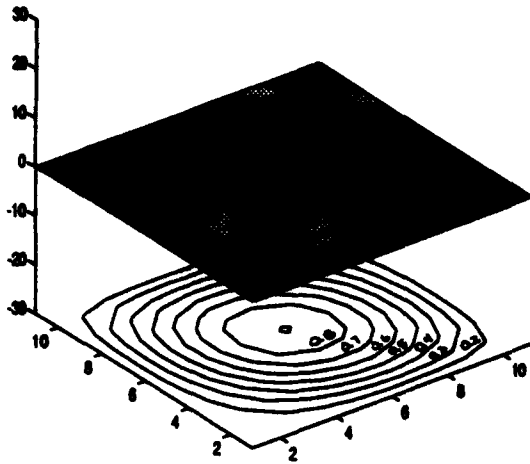
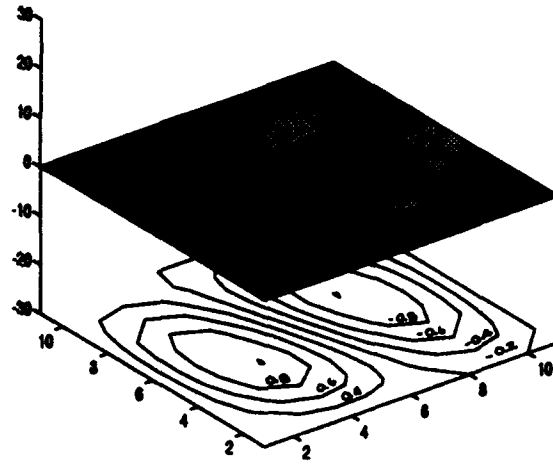First Mode Shape

Second Mode Shape

Third Mode Shape

Fourth Mode Shape

Fig. 4.9 Mode Shapes for Panel # 2, Simply Supported Boundary
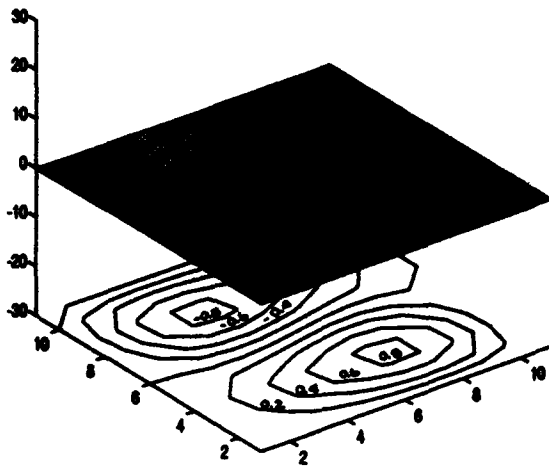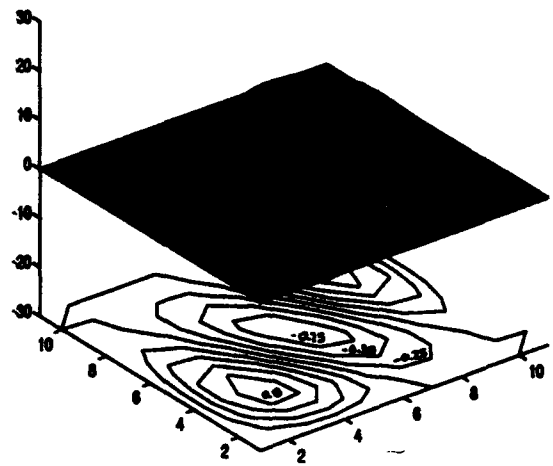Condition [-45°/45°]$_s$ laminate, h/R = 1/20, b/h = 20

A complete set of results of this analysis including the first four natural frequencies, for both ply orientation and the specified boundary conditions, is given in the following tables.

b/h = 10	Mode # 1	Mode # 2	Mode # 3	Mode # 4
h/R = 1/20	10702.72	18977.13	20461.18	20498.97
h/R = 1/50	10482.24	18649.47	20375.15	20419.14
h/R = 1/200	10441.45	18542.59	20309.14	20362.41

b/h = 15	Mode # 1	Mode # 2	Mode # 3	Mode # 4
h/R = 1/20	5685.29	9374.52	13598.58	13617.48
h/R = 1/50	5127.56	9360.28	13568.24	13586.38
h/R = 1/200	5016.13	9266.70	13500.43	13549.20

b/h = 20	Mode # 1	Mode # 2	Mode # 3	Mode # 4
h/R = 1/20	4016.82	5524.13	10205.80	10397.55
h/R = 1/50	3124.43	5497.42	9314.28	10269.94
h/R = 1/200	2919.27	5429.79	9088.64	10193.29

b/h = 30	Mode # 1	Mode # 2	Mode # 3	Mode # 4
h/R = 1/20	2760.3	3036.1	4904.9	5698.4
h/R = 1/50	1773.2	2563.2	4754.5	4988.8
h/R = 1/200	1355.5	2524.7	4417.8	4708.8

b/h = 40	Mode # 1	Mode # 2	Mode # 3	Mode # 4
h/R = 1/20	1900.36	2702.33	2842.59	4030.63
h/R = 1/50	1400.27	1524.24	2737.03	3137.14
h/R = 1/ 200	809.38	1442.29	2613.72	2836.48

b/h = 50	Mode # 1	Mode # 2	Mode # 3	Mode # 4
h/R = 1/20	1575.89	1931.45	2477.51	3127.58
h/R = 1/ 50	1071.26	1266.30	1853.52	2233.47
h/R = 1/200	570.72	935.18	1757.98	1838.85

Table 4-7 First four Natural Frequencies, Panel # 2, Simply
Supported Boundary Condition, $[0^o/90^o]_s$ ply orientation.

b/h = 10	Mode #1	Mode #2	Mode #3	Mode #4
h/R = 1/20	13672.26	22404.69	26239.22	29104.94
h/R = 1/50	12349.65	22138.28	25899.37	28886.96
h/R = 1/200	12092.08	22076.65	25819.76	28839.93

b/h = 15	Mode #1	Mode #2	Mode #3	Mode #4
h/R = 1/20	8840.34	11772.55	14737.46	18408.56
h/R = 1/50	6468.87	11367.77	13818.49	17716.12
h/R = 1/200	5919.98	11232.03	13698.42	17578.29

b/h = 20	Mode #1	Mode #2	Mode #3	Mode #4
h/R = 1/20	8285.94	7427.99	10384.23	12037.38
h/R = 1/50	4389.53	6935.45	8615.55	11019.53
h/R = 1/200	3504.12	6717.43	8379.37	10777.59

b/h = 30	Mode #1	Mode #2	Mode #3	Mode #4
h/R = 1/20	3668.95	6254.74	6431.54	8701.83
h/R = 1/50	3165.36	3459.07	4667.79	5666.27
h/R = 1/200	1720.89	3167.73	4026.06	5187.10

b/h = 40	Mode #1	Mode #2	Mode #3	Mode #4
h/R = 1/20	2414.96	3685.05	5469.36	5625.56
h/R = 1/50	2107.75	2872.94	3512.95	3618.75
h/R = 1/ 200	1135.68	1859.18	2373.24	3051.14

b/h = 50	Mode #1	Mode #2	Mode #3	Mode #4
h/R = 1/20	1902.79	2678.49	3873.12	4603.97
h/R = 1/ 50	1463.64	2356.94	2756.15	3119.88
h/R = 1/200	906.12	1245.63	1605.09	2039.39

Table 4-8 First four Natural Frequencies, Panel #2, Simply Supported Boundary Condition, $[-45^{o}/+45^{o}]_S$ ply orientation.

The next figures show the behavior of the second, third and fourth mode. They were constructed using the data above.

Figs 4.10 and 4.11 show the behavior of the frequencies for the second mode under the boundary condition considered. According to these figures, the frequencies for the $[-45^O/+45^O]_S$ laminate are higher than the ones for the $[0^O/90^O]_S$ ply orientation. The panel stiffness is higher in the $[-45^O/+45^O]_S$ laminate as indicated previously. Also the effect of the through the thickness shear becomes evidently higher for the $[-45^O/+45^O]_S$ laminate.

Also from fig 4.11, for values b/h > 20 (deeper and thinner shells) through the thickness shear effects decreased but the curvature effects becomes significant. Also for deeper shells, b/h > 50, on the same value of curvature, the behavior of the curve seems to reach a specific value, for both orientations, this value should correspond to the frequency of a shell with no shear.
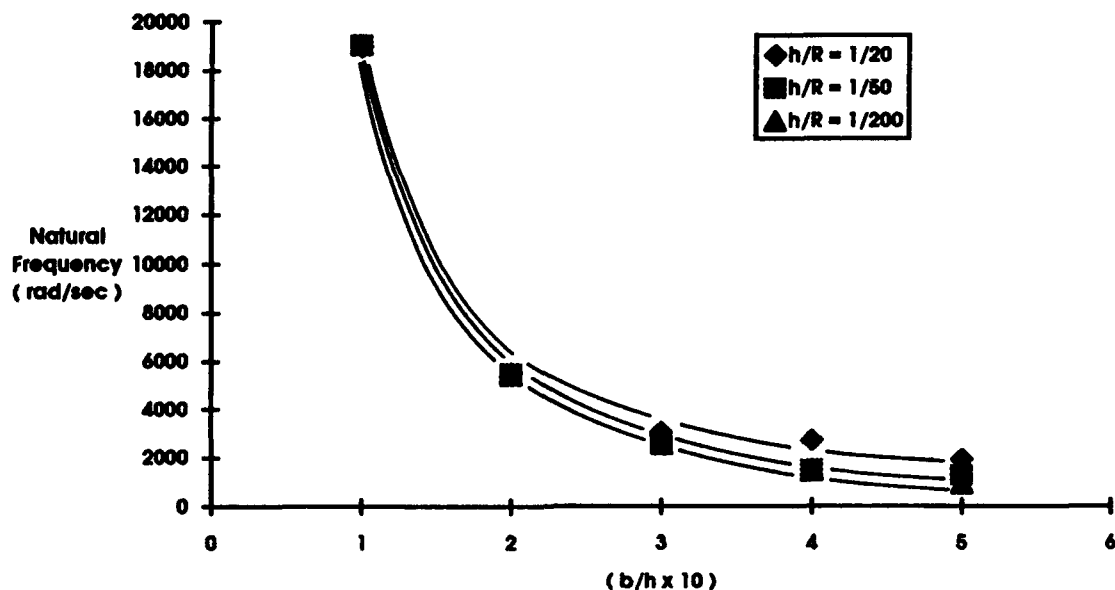

Fig 4.10   Curvature Effects for the Second Natural Frequency, Panel # 2,
            Simply Supported Boundary Condition, $[0^O/90^O]_S$ laminate.
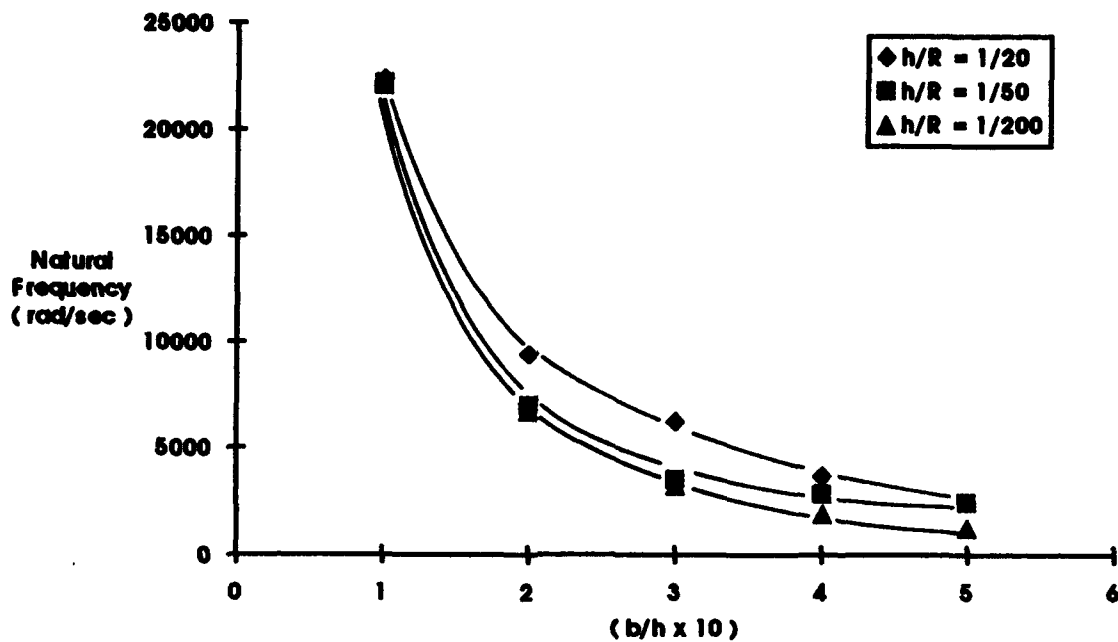
Fig 4.11 Curvature Effects for the Second Natural Frequency, Panel # 2
Simply Supported Boundary Condition, [-45°/+45°]$_S$ laminate

Figs 4.12 and 4.13 show the behavior of the frequencies for the third mode. According to these figures the frequencies for the [-45°/+45°]$_S$ laminate are higher than the ones for the [0°/90°]$_S$ ply orientation. The effect of the through the thickness shear is also evidently higher in the [-45°/+45°]$_S$ than in the [0°/90°]$_S$ laminate. The effect of curvature is practically negligible for the [0°/90°]$_S$ laminate (since the curves are very close, but in the [-45°/+45°]$_S$ laminate, it becomes important.

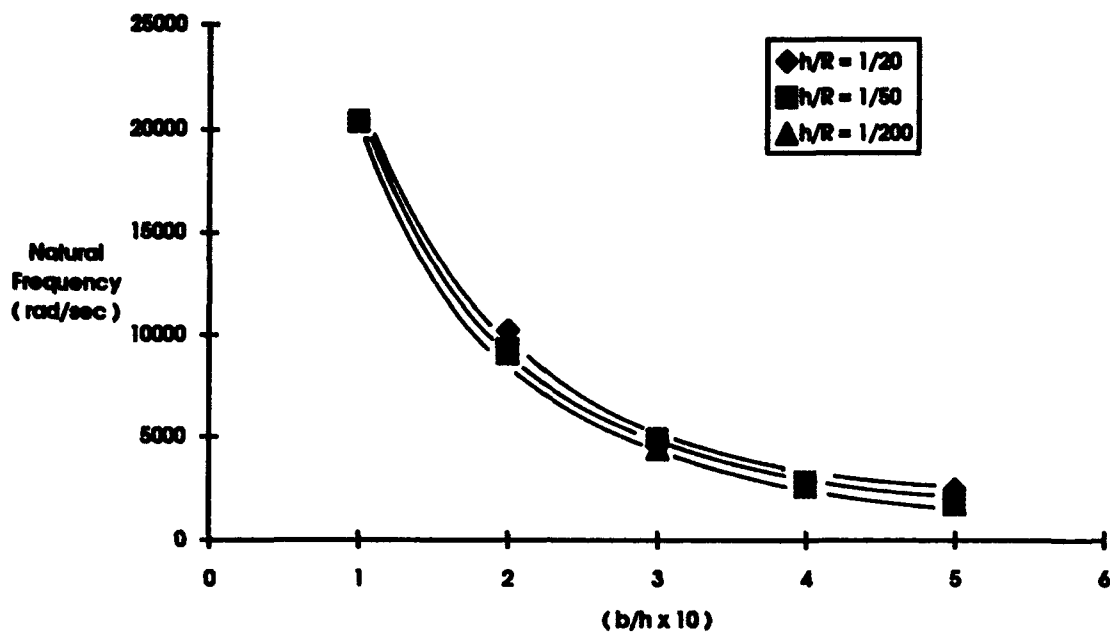The same trends are also seen in figs. 4.14 and 4.15, for the fourth natural frequency.

Fig 4.12 Curvature Effects for the Third Natural Frequency, Panel # 2,
Simply Supported Boundary Condition, [0°/90°]$_S$ laminate

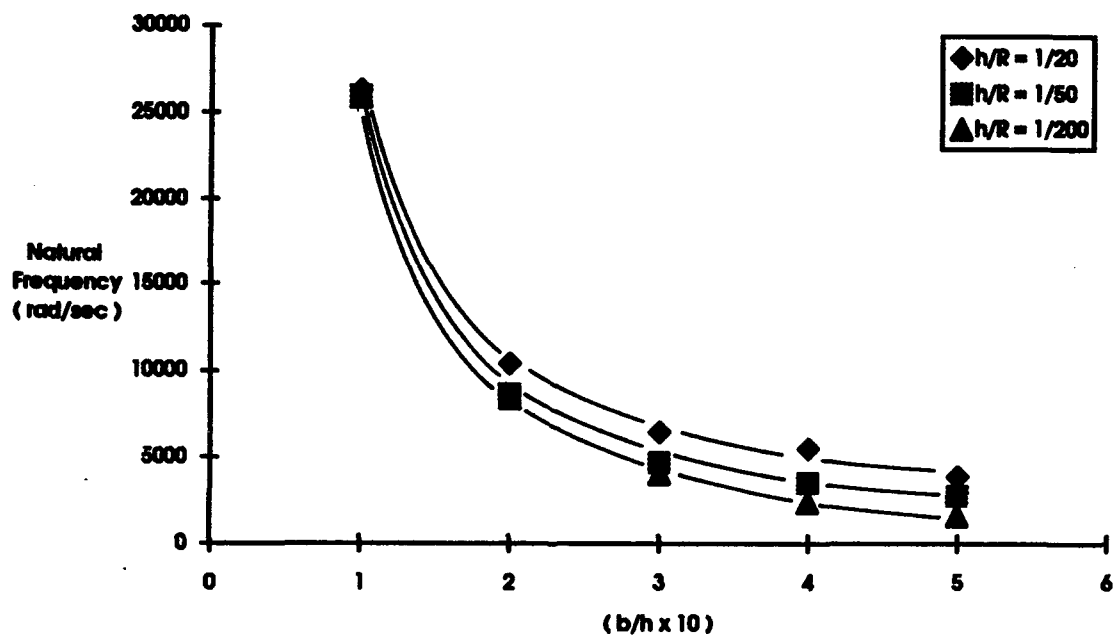Fig 4.13 Curvature Effects for the Third Natural Frequency, Panel # 2
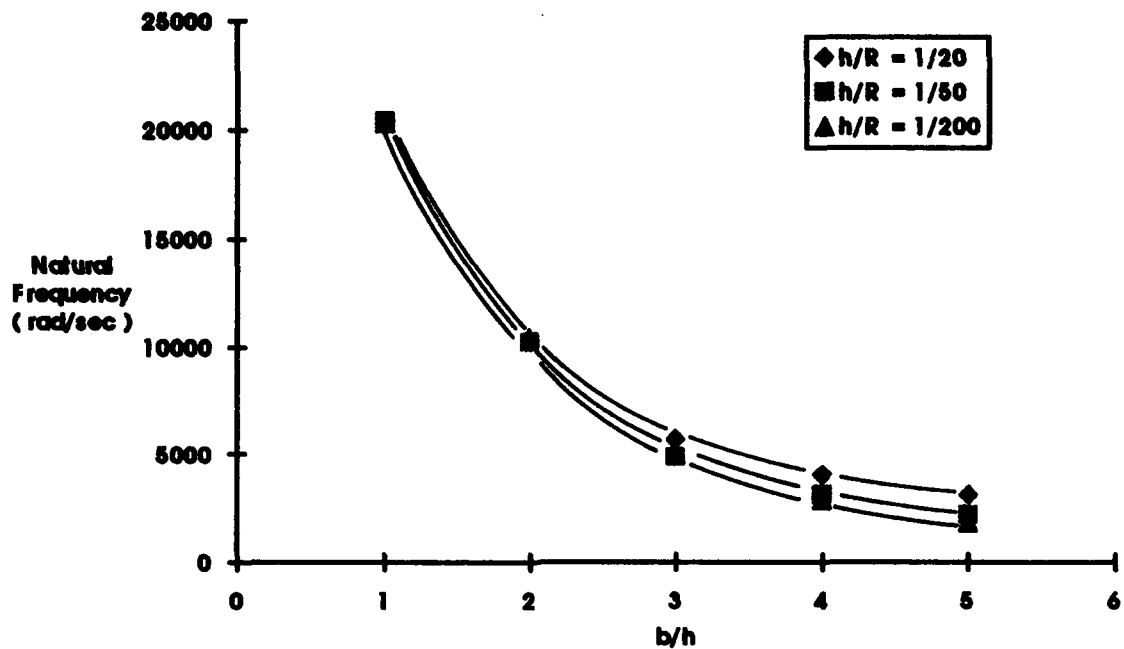Simply Supported Boundary Condition, [-45°/+45°]$_S$ laminate

Fig 4.14 Curvature Effects for the Fourth Natural Frequency, Panel # 2
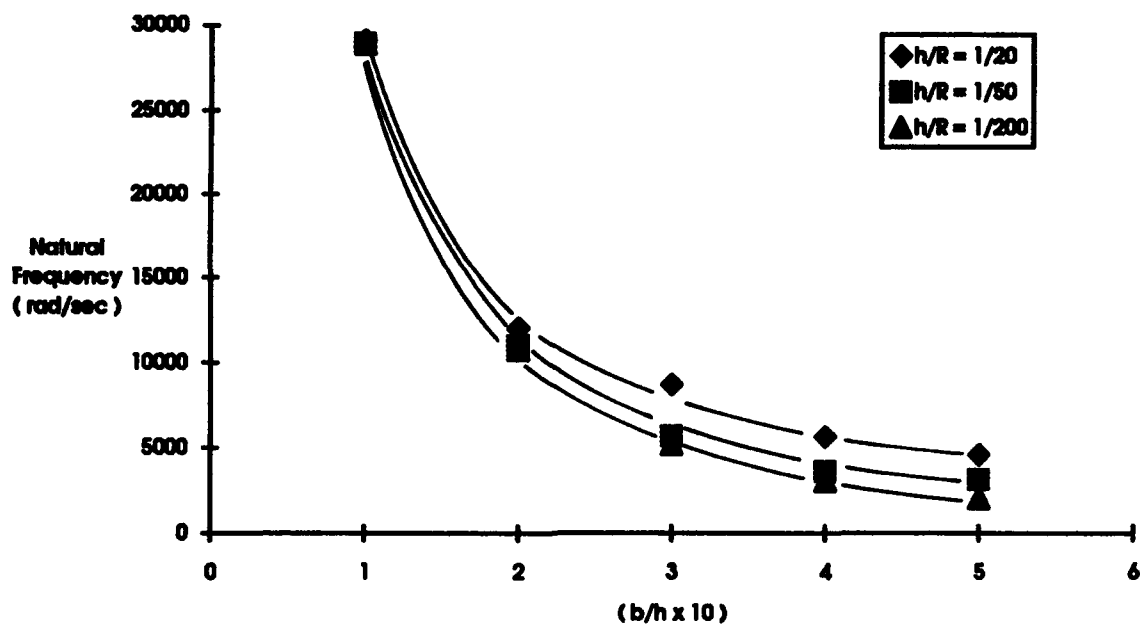Simply Supported Boundary Condition, $[0^o/90^o]_S$ laminate

Fig 4.15 Curvature Effects for the Fourth Natural Frequency, Panel # 2
Simply Supported Boundary Condition, $[-45^o/+45^o]_S$ laminate

Also comparisons can be made between the ply orientations for the specific value of h/R = 1/20; Figs 4.16, 4.17 and 4.18 show the behavior of the second, third and fourth mode respectively.

It is noticed that the frequency magnitude for the $[-45^o/+45^o]_S$ ply orientation is higher than the corresponding values for the $[0^o/90^o]_S$ laminate for the second, third and fourth modes. In addition, for b/h > 30, the difference in frequency between both orientations is very small.
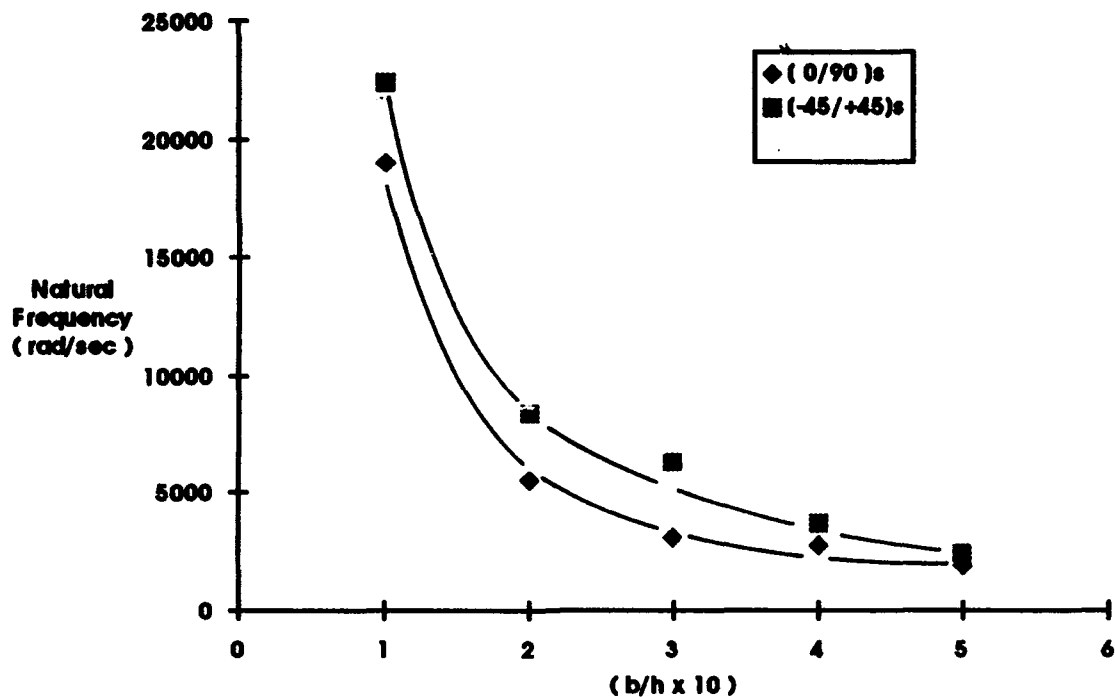

Fig 4.16 Comparisons between $[0^o/90^o]_S$ and $[-45^o/+45^o]_S$ laminate, Panel # 2
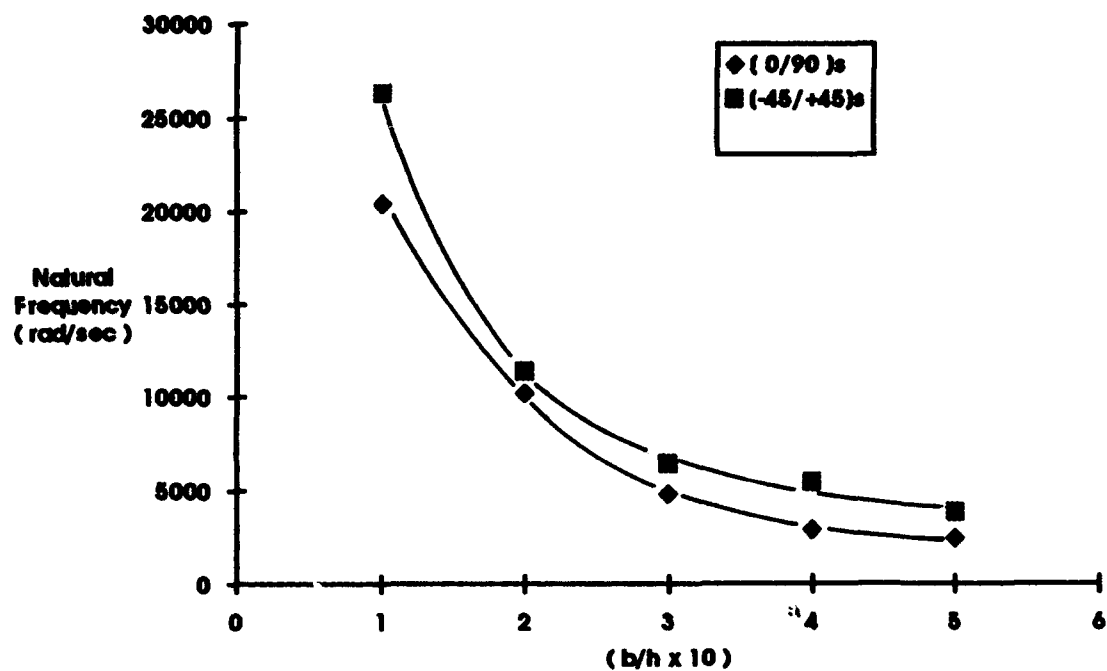Second Natural Frequency, Simply Supported Boundary Condition

Fig 4.17 Comparisons between $[0^o/90^o]_S$ and $[-45^o/+45^o]_S$ laminate, Panel # 2
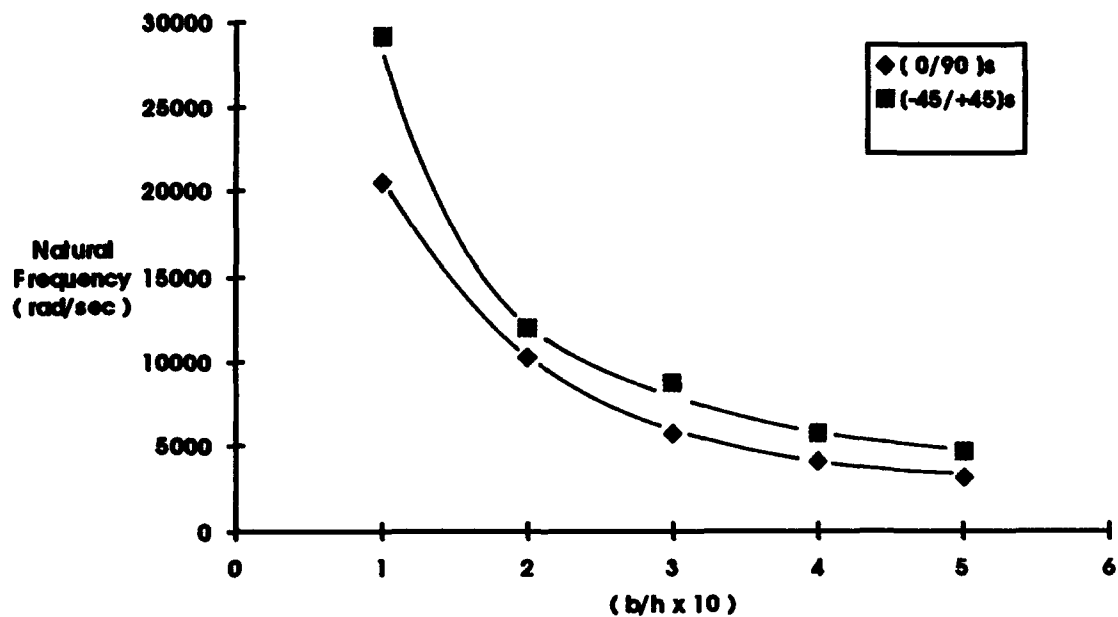Third Natural Frequency, Simply Supported Boundary Condition

Fig 4.18 Comparisons between $[0^o/90^o]_S$ and $[-45^o/+45^o]_S$ laminate, Panel # 2
Fourth Natural Frequency, Simply Supported Boundary Condition

Simply Supported-Free Boundary Condition.

The next case investigated was the Simply Supported-Free-Simply Supported-Free Boundary Condition. The DOF applied in this boundary condition were specified in Table 4-4. DSHELL again showed flexibility in getting the eigenvalues and the corresponding mode shapes for this boundary condition, so the calculations were straight forward.

Following the pattern used with the previous boundary condition, the same thickness to radius of curvature ratios, h/R, were used (1/20, 1/50, 1/200) for specific values of circumferential length to thickness ratios b/h (10, 20, 30, 40 and 50).

The next tables, Table 4-9 and Table 4-10 respectively, show the magnitude of the first four natural frequencies using DSHELL finite element program for both ply orientation $[0^o/90^o]_s$, and $[-45^o/+45^o]_s$.

b/h = 10 (1)	Mode # 1	Mode # 2	Mode # 3	Mode # 4
h/R = 1/20	6069.1	9043.4	15759.8	16582.6
h/R = 1/50	5240.8	7259.0	15240.6	16386.6
h/R = 1/200	5063.2	6875.7	15226.7	16334.4

b/h = 15 (2)	Mode # 1	Mode # 2	Mode # 3	Mode # 4
h/R = 1/20	3961.8	6688.1	8052.4	9365.8
h/R = 1/50	2764.7	4129.6	7896.7	9256.8
h/R = 1/200	2408.6	3393.3	7605.5	9152.6

b/h = 20 (3)	Mode # 1	Mode # 2	Mode # 3	Mode # 4
h/R = 1/20	3181.3	4469.7	5575.2	5796.2
h/R = 1/50	1941.3	3125.6	4862.5	5504.1
h/R = 1/200	1431.2	2075.9	4745.3	5490.3

b/h = 30 (4)	Mode # 1	Mode # 2	Mode · # 3	Mode # 4
h/R = 1/20	1965.3	2497.1	2964.8	3910.8
h/R = 1/50	1375.8	2162.0	2494.3	2676.8
h/R = 1/200	731.4	1122.4	2197.5	2612.5

b/h = 40 (5)	Mode # 1	Mode # 2	Mode # 3	Mode # 4
h/R = 1/20	1162.4	2033.7	2104.3	2585.0
h/R = 1/50	1054.2	1228.2	1654.0	2162.4
h/R = 1/ 200	502.5	819.1	1259.1	1530.1

b/h = 50 (6)	Mode # 1	Mode # 2	Mode # 3	Mode # 4
h/R = 1/20	787.8	1503.3	1688.0	1720.2
h/R = 1/ 50	636.4	1047.4	1327.9	1527.7
h/R = 1/200	404.2	699.0	814.7	1011.8

Table 4-9 First Four Natural Frequencies using DSHELL, Panel # 2, $[0^o/90^o]_S$ laminate, Simply Supported-Free Boundary Condition.

As expected, by using this boundary condition, the frequencies obtained are lower than the values for the previous boundary. For both laminates , $[0^o/90^o]_S$ and $[-45^o/+45^o]_S$, the values of frequencies obtained are about 50% the corresponding value of frequency

calculated for the Simply Supported all edges boundary condition.

b/h = 10 (1)	Mode # 1	Mode # 2	Mode # 3	Mode # 4
h/R = 1/20	6851.8	10775.6	18488.0	18814.4
h/R = 1/50	5865.1	9824.4	18172.9	18412.6
h/R = 1/200	5665.9	9644.1	18127.6	18287.9

b/h = 15 (2)	Mode # 1	Mode # 2	Mode # 3	Mode # 4
h/R = 1/20	4786.3	6671.5	9457.4	10410.5
h/R = 1/50	3205.8	5110.7	9250.4	9352.1
h/R = 1/200	2805.9	4741.0	9111.4	9304.2

b/h = 20 (3)	Mode # 1	Mode # 2	Mode # 3	Mode # 4
h/R = 1/20	4147.1	4836.3	6145.7	7085.6
h/R = 1/50	2306.3	3415.1	5671.7	5852.6
h/R = 1/200	1702.4	2835.8	5455.7	5690.7

b/h = 30 (4)	Mode # 1	Mode # 2	Mode # 3	Mode # 4
h/R = 1/20	2310.2	3411.5	4290.7	4353.3
h/R = 1/50	1767.3	2224.6	2865.7	3263.9
h/R = 1/200	883.8	1402.5	2616.1	2734.4

b/h = 40 (5)	Mode # 1	Mode # 2	Mode # 3	Mode # 4
h/R = 1/20	1448.2	2526.4	2916.6	3175.3
h/R = 1/50	1262.2	1586.9	2194.4	2232.0
h/R = 1/ 200	612.5	906.2	1582.9	1608.2

b/h = 50 (6)	Mode # 1	Mode # 2	Mode # 3	Mode # 4
h/R = 1/20	951.5	1757.5	1990.1	2413.3
h/R = 1/ 50	760.8	1427.0	1713.0	1828.2
h/R = 1/200	503.9	692.8	1067.5	1112.9

Table 4-10 First Four Natural Frequencies using DSHELL, Panel # 2,
[-45°/+45°]$_S$ laminate, Simply Supported-Free Boundary Condition

The fundamental mode will be discussed next since it is most important in the analysis.

Figure 4.19 shows the effect of curvature h/R on the fundamental frequency for panel # 2,

[0°/90°]$_S$ ply orientation. As it is seen, as the curvature increases, the panel becomes deeper and stiffer and the natural frequencies increase.

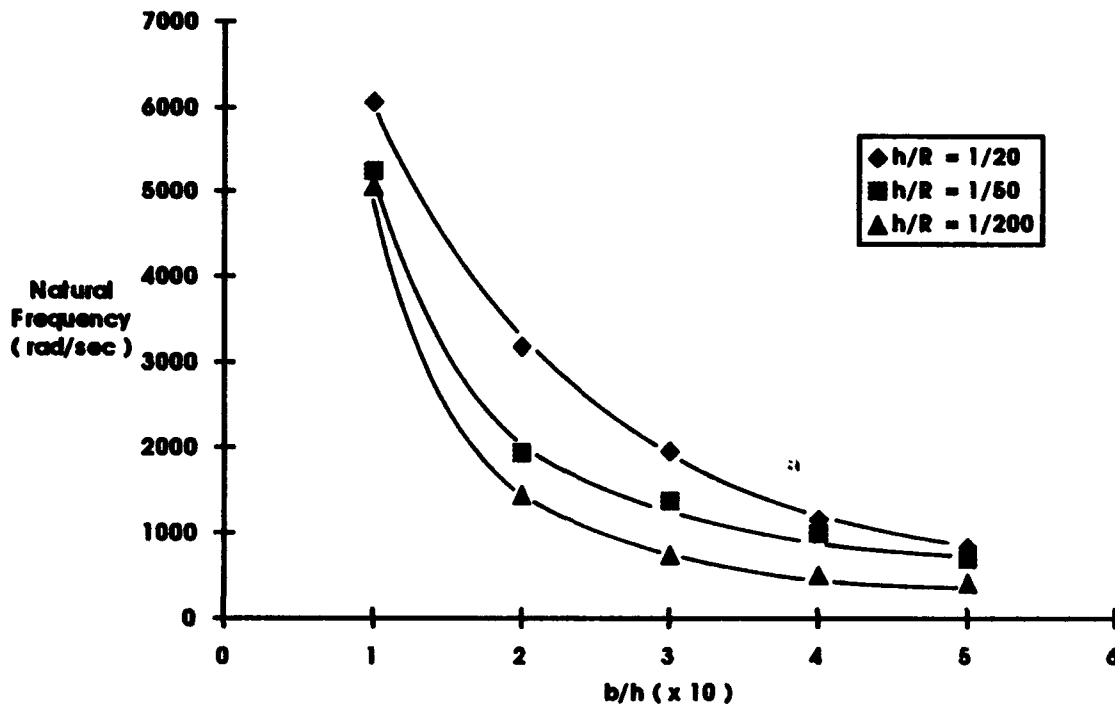Fig 4.19 Curvature Effects on the Fundamental Frequency, [0°/90°]$_S$
ply orientation, Simply Supported-Free Boundary Condition

Some tendencies are also recognized. The natural frequencies are seen to increase as h/R is increased due to the membrane and bending coupling. Also, the effect of increasing the span to thickness ratio, b/h, is seen to lower the frequencies. The same behavior was noticed for the [-45°/+45°]$_S$ laminate, Figure 4-20. Both figures present basically the same tendencies except that, the curves for the [-45°/+45°]$_S$ laminate are higher in magnitude than the corresponding curve for the [0°/90°]$_S$ laminate as indicated previously.
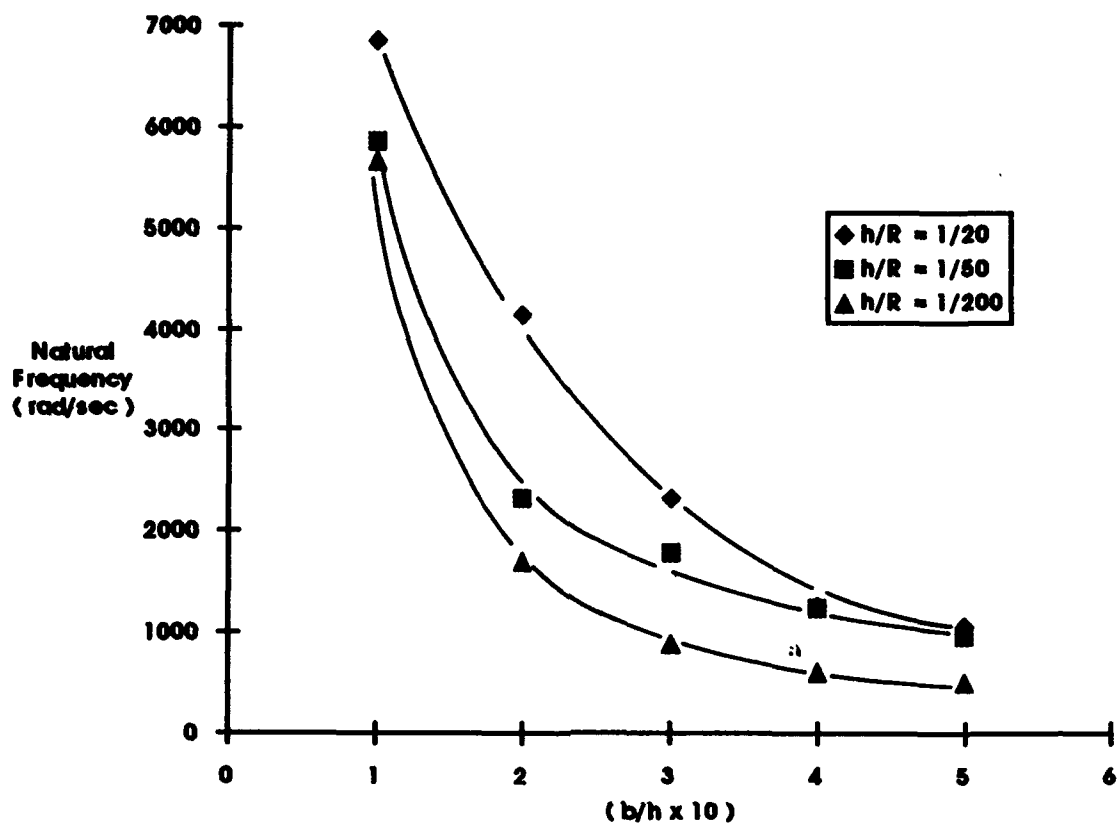
Fig 4.20 Curvature Effects on the Natural Frequencies, Panel # 2, $[-45^{o}/+45^{o}]_s$
ply orientation, Simply Supported-Free Boundary Condition

The next figure shows the difference in natural frequencies for both laminates. Again, the

natural frequencies for the $[-45^{o}/+45^{o}]_s$ laminate are higher than the value for the

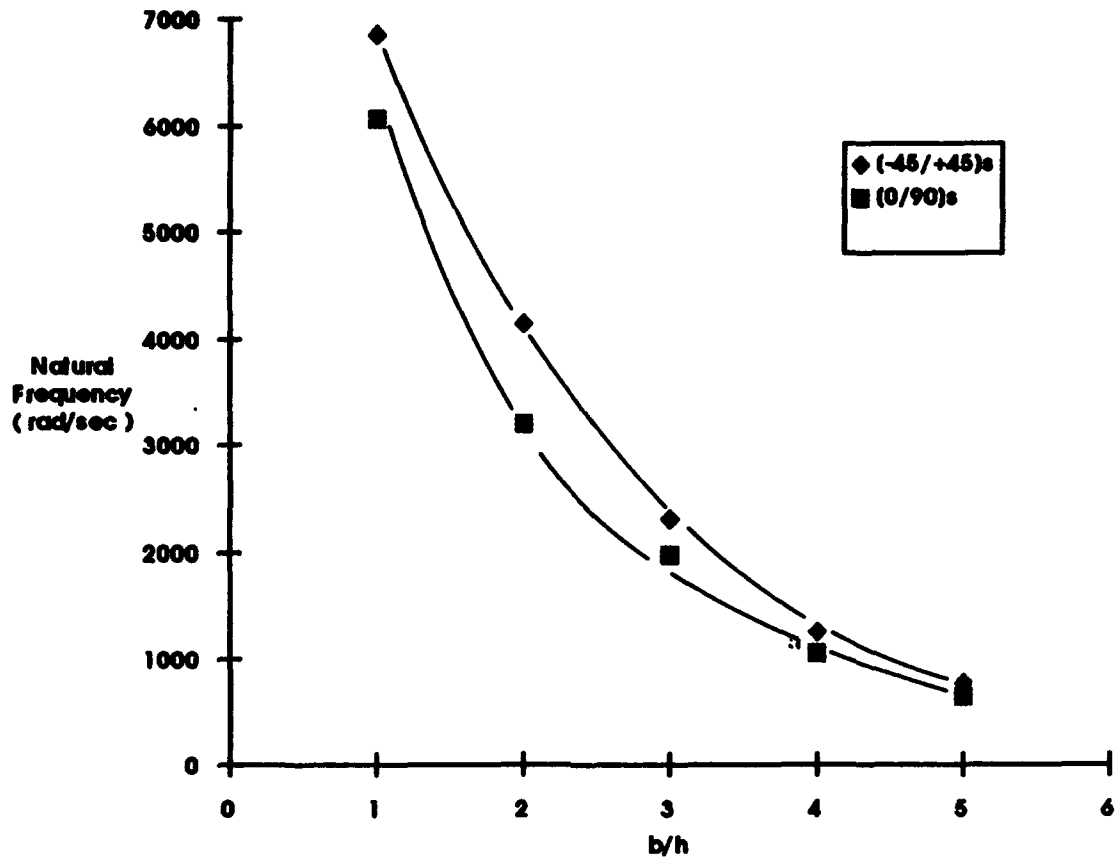$[0^{o}/90^{o}]_s$ orientation due to the higher stiffness and thickness effects in the first layup.

Fig. 4.21   Comparison in the First Natural Frequency between the
$[0^o/90^o]_S$ and $[-45^o/+45^o]_S$ ply orientations, Simply
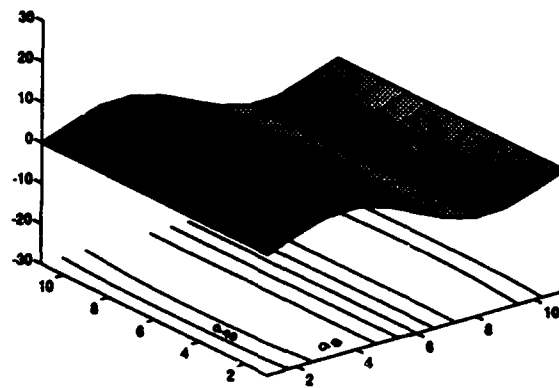Supported-Free Boundary Condition, h/R = 1/20

Also from this figure it can be seen that for values b/h < 30, the variation between the two

frequencies is significant but as b/h increases, the comparison for both laminates converge.

Although only the first natural frequency has been included in the previous analysis (fig

4.19), the mode shapes corresponding to the first four natural frequency for the $[0^o/90^o]_S$

and $[-45^o/+45^o]_S$ ply orientation with simply supported-free boundary condition are
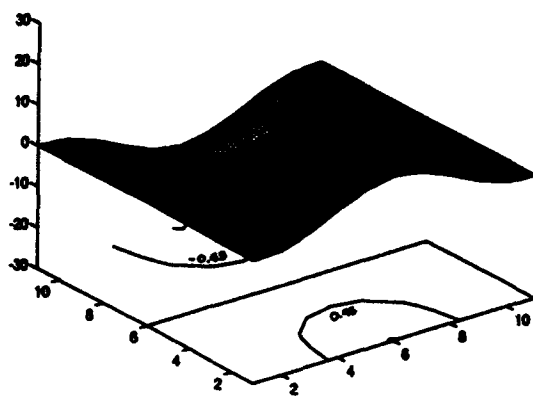
included in the next figures.

From figure 4.22, it can be seen that the first mode shape for the $[0^o/90^o]_s$ ply orientation, is symmetric, the second, third and fourth mode are antisymmetric.
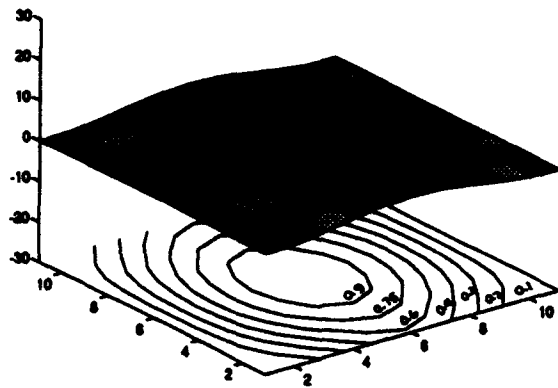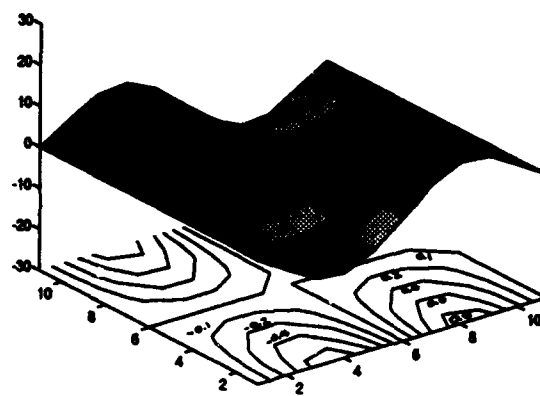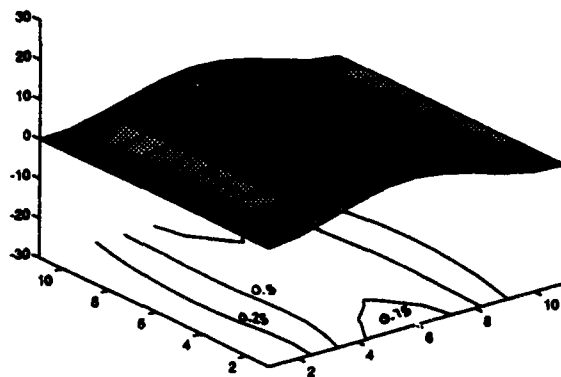
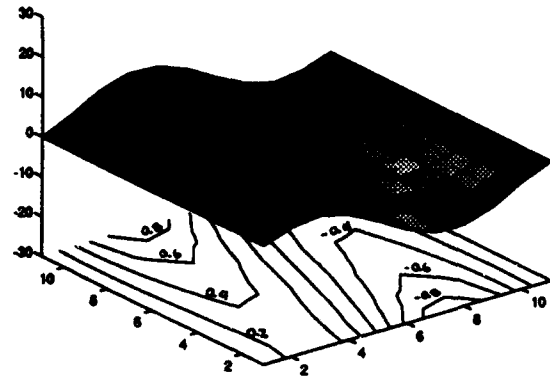

First Mode Shape   Second Mode Shape

Third Mode Shape   Fourth Mode Shape

Fig 4.22 Mode Shapes for Panel # 2, $[0^o/90^o]_s$ ply orientation, b/h = 20, h/R = 1/20, Simply Supported-Free Boundary Condition.
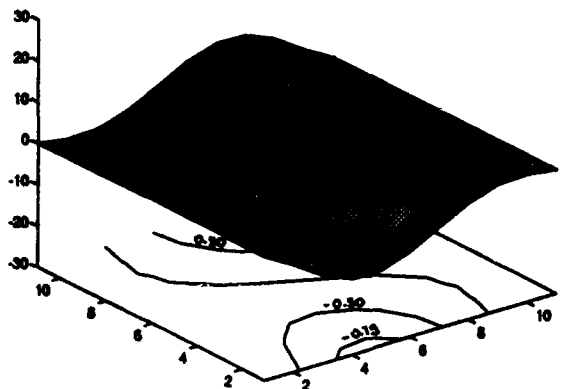
From figure 4.23, it can be seen that the first mode shape for the [-45°/+45°]$_S$ ply

orientation, is symmetric, the second, third and fourth mode are antisymmetric, is the same
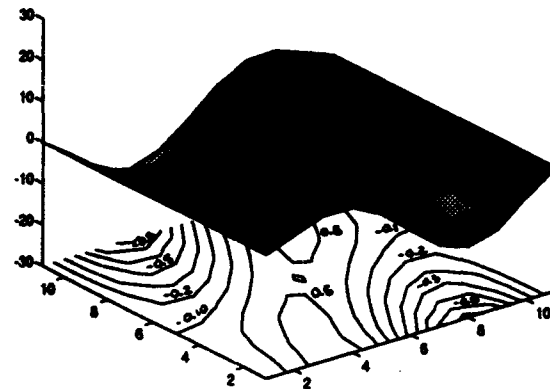
as the [0°/90°]$_S$ ply orientation.

First Mode Shape

Second Mode Shape

Third Mode Shape

Fourth Mode Shape

Fig 4.23   Mode Shapes for Panel # 2, [-45°/+45°] ply orientation, b/h = 20,
h/R =1/20, Simply Supported-Free BoundaryCondition

In the following figures the curvature effects on the second, third and fourth frequencies

for both ply orientation are shown. Figures 4.24 and 4.25 present the curvature effects

on the second natural frequency for both laminates respectively. For both laminates, the

frequency is seen to increase as h/R increases, but the frequency decreases by increasing

the distance between the boundaries. Also the frequencies for the $[-45^o/+45^o]_s$ ply

orientation are higher than the corresponding values for the $[0^o/90^o]_s$ laminate, for the

four frequencies, through all interval b/h analyzed.
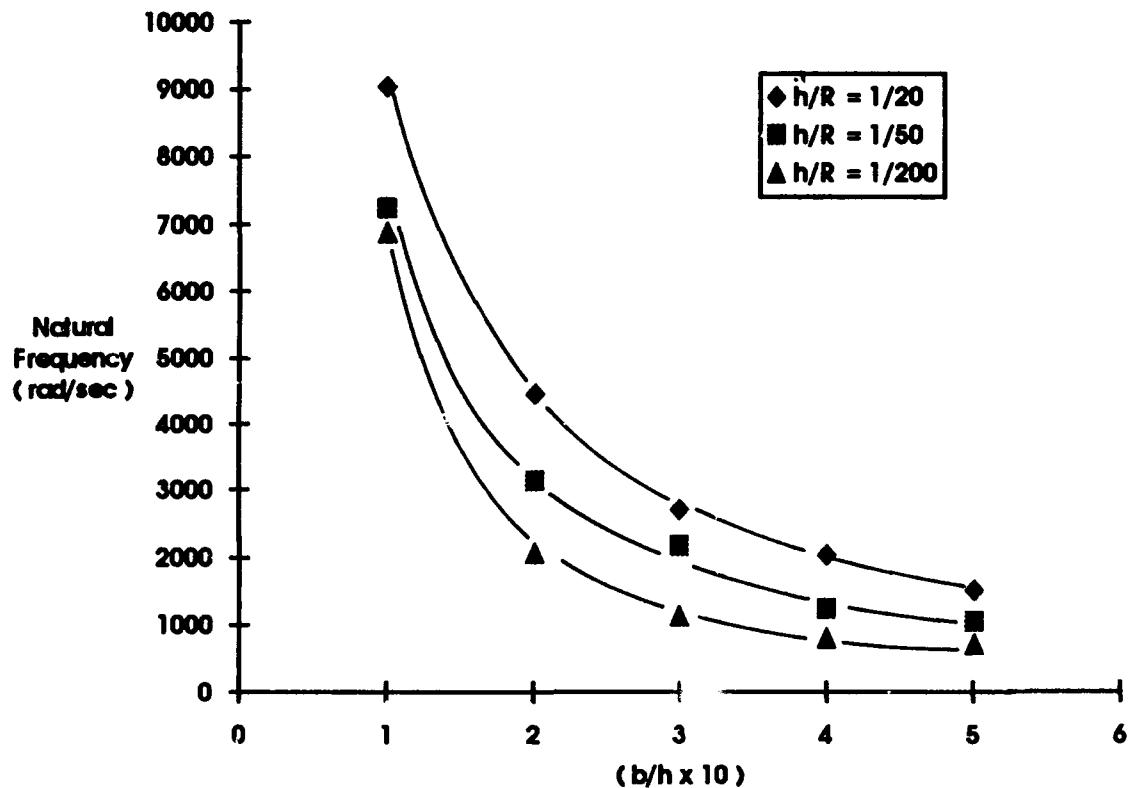

Fig 4.24 Curvature Effects on the Second Natural Frequency, $[0^o/90^o]_s$
ply orientation, Simply Supported-Free Boundary Condition

In addition, the difference in frequency among the three ratios of curvature seems to remain constant for each ply orientation along the interval b//h study, although for closed boundaries, b/h < 20, this difference is larger in the $[0^o/90^o]_S$ ply orientation. If these figures are compared with the respective ones obtained for the previous boundary (figures 4.10 and 4.11), it is seen that the difference in frequency among the three ratios h/R studied, for each b/h value, is higher in the present boundary condition case for both laminates than the corresponding ply orientation in the previous boundary.
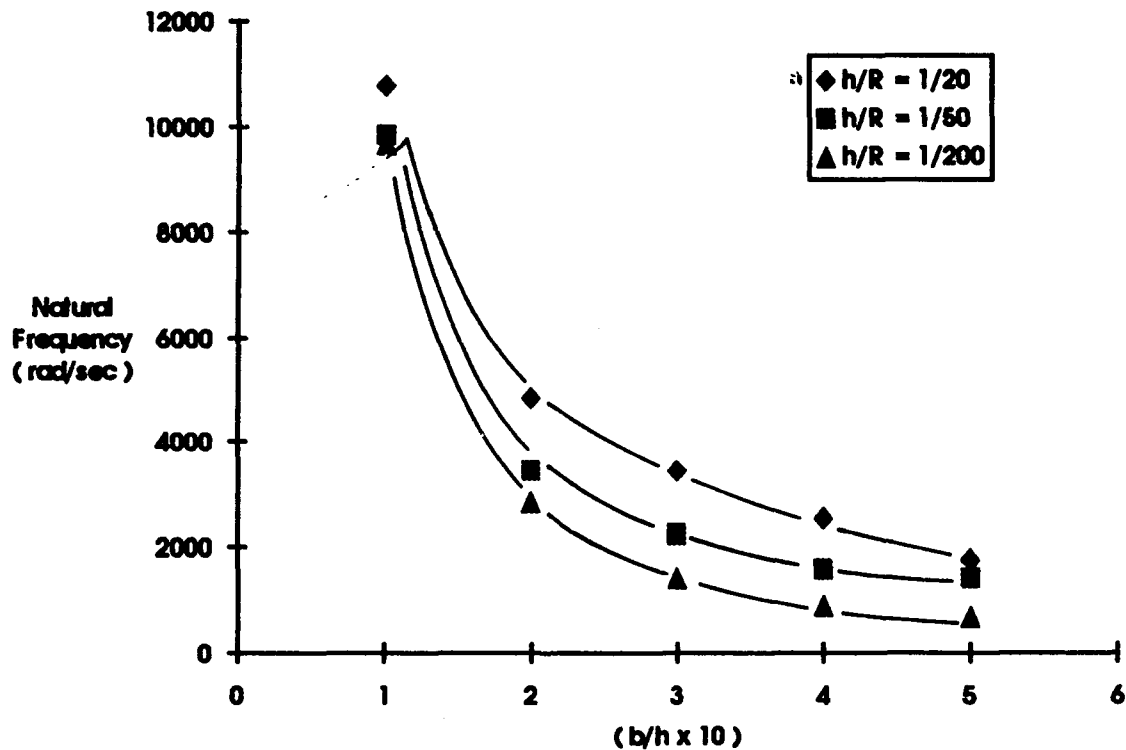

Fig 4.25   Curvature Effects on the Second Natural Frequency, $[-45^o/+45^o]_S$ ply orientation, Simply Supported-Free Boundary Condition

Figures 4.26 and 4.27 show the curvature effect on the third natural frequency for both
laminates respectively; frequency increases as h/R increases too, but it decreases by
increasing the distance between boundaries.   Also, the effect of the boundary condition is
noticed, by comparing these figures with figures 4.12 and 4.13, corresponding to the same
frequency but simply supported all edges, the frequency magnitudes in the present case are
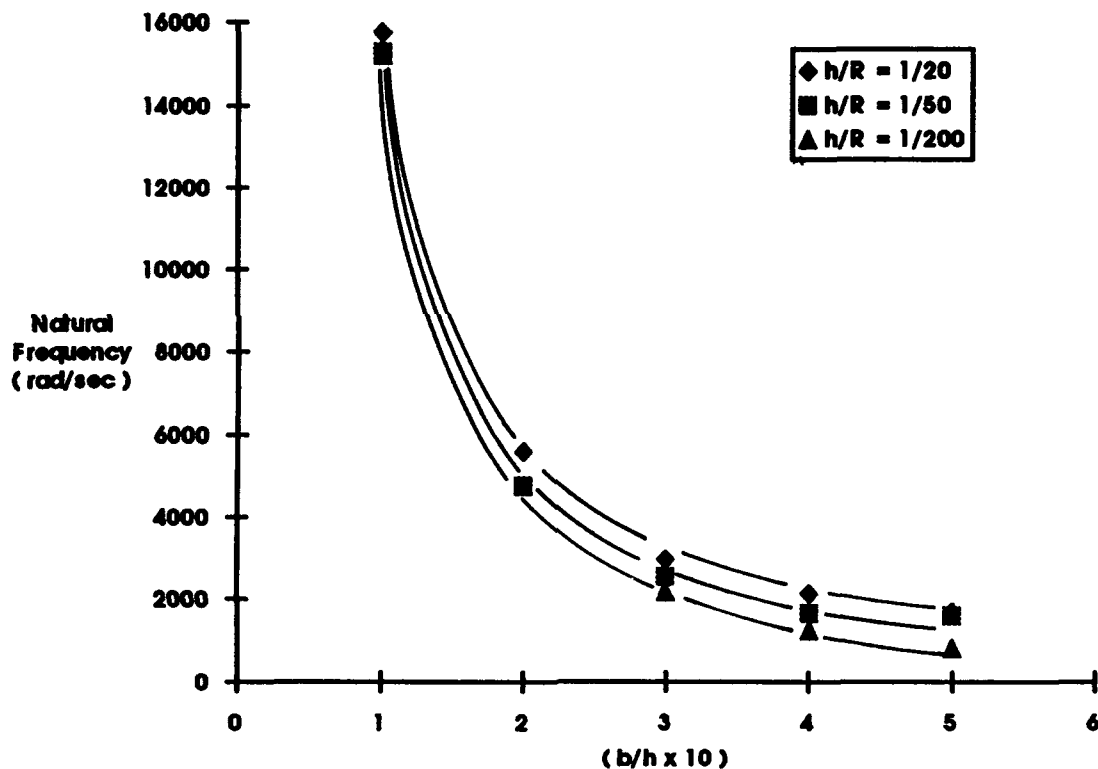lower than the values for frequencies obtained for the previous boundary.

Fig 4.26 Curvature Effects on the Third Natural Frequency, $[0^o/90^o]_s$
laminate, Simply Supported-Free Boundary Condition

Fig 4.27 Curvature Effects on the Third Natural Frequency, $[-45^o/+45^o]_S$
ply orientation, Simply Supported-Free Boundary Condition

Figures 4.28 and 4.29 show the curvature effect on the fourth natural frequency for both

laminates respectively; frequency increases as h/R increases too, but it decreases by

increasing the distance between boundaries. These curves follow exactly the same trend

seen in the third mode, the effects of curvature are not observable at the shallower end of

the composite (b/h < 20), specially in the $[0^o/90^o]_S$ ply orientation, but they are more

evident at the deeper end in the $[-45^o/+45^o]_S$ ply orientation.

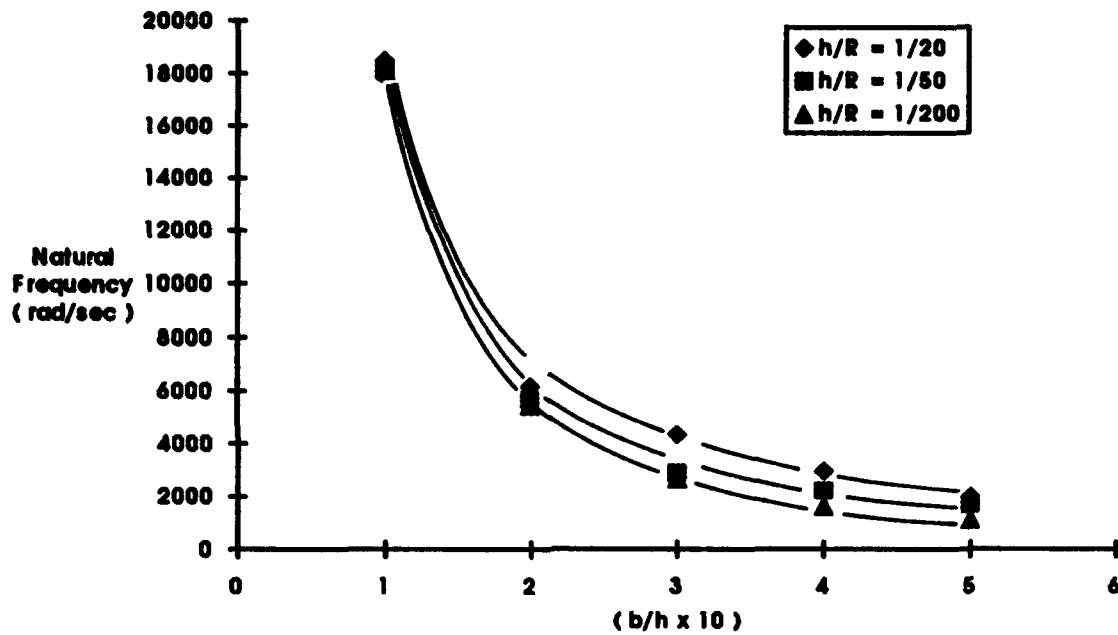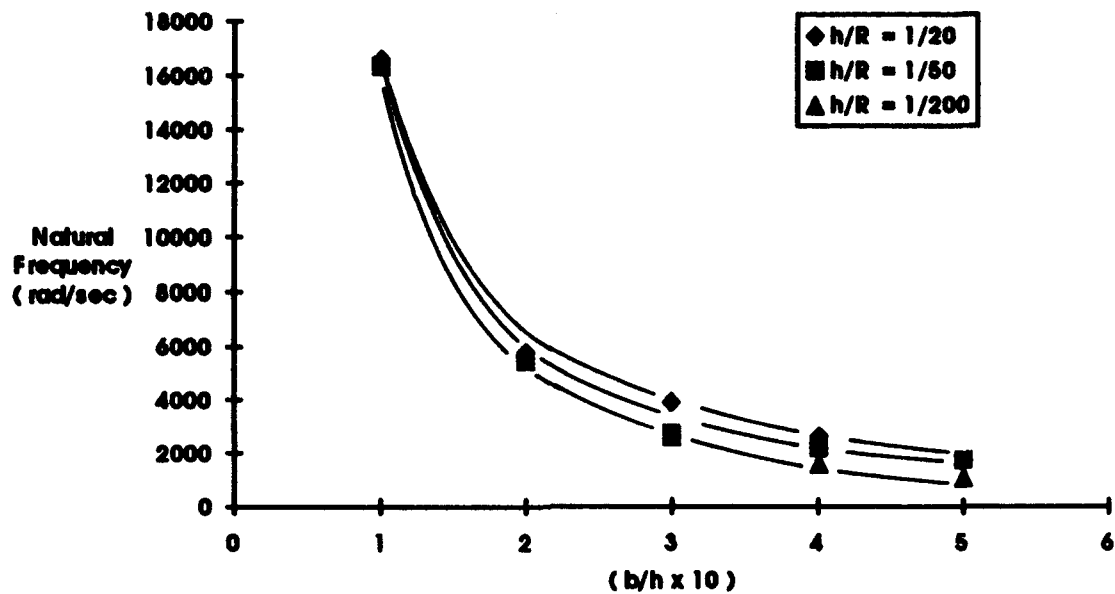Fig 4.28 Curvature Effects on the Fourth Natural Frequency, $[0^o/90^o]_s$ laminate, Simply Supported-Free Boundary Condition
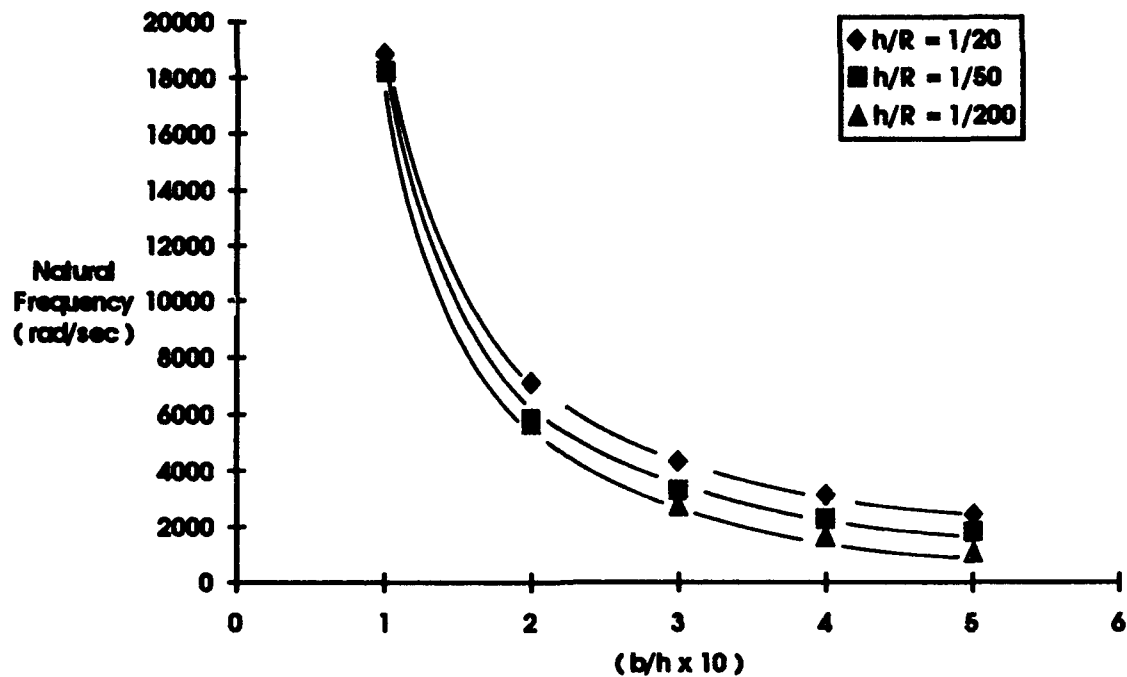

Fig 4.29 Curvature Effects on the Fourth Natural Frequency, $[-45^o/+45^o]_s$ ply orientation, Simply Supported-Free Boundary Condition

Following the analysis made with the previous boundary condition, comparisons between both ply orientations can also be made for h/R = 1/20.

Figures 4.30, 4.31 and 4.32 show the difference between the $[0^o/90^o]_S$ and $[-45^o/+45^o]_S$ ply orientation for the second, third and fourth natural frequency for the simply supported-free boundary condition. It is seen that the natural frequencies for the $[-45^o/+45^o]_S$ laminate are higher than the corresponding frequencies for the $[0^o/90^o]_S$ ply orientation, this difference is about 20%, for the three cases, and it remains approximately constant through all the interval b/h analyzed. Also, it is evident that the effect of the through the thickness shear on the $[-45^o/+45^o]_S$ ply orientation is greater, specially at the shallower end of the composite, although this effect becomes negligible as the deepness is increased.
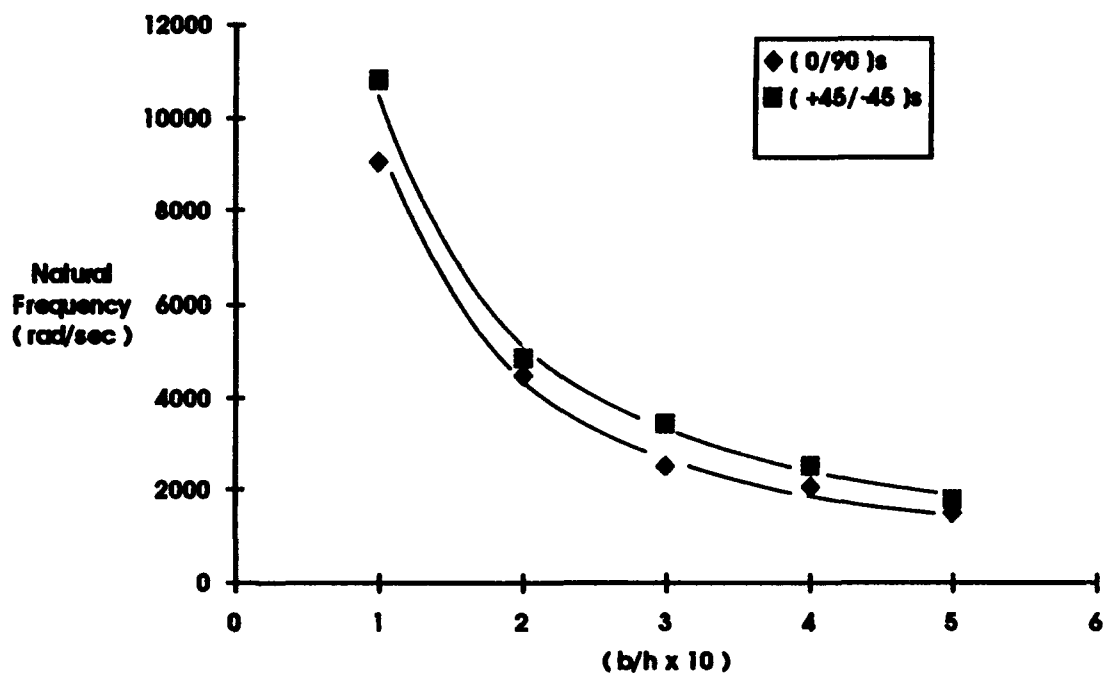
Fig 4.30 Comparison between $[0^o/90^o]_S$ and $[-45^o/+45^o]_S$ ply orientation, Second Natural Frequency, Simply Supported-Free Boundary Condition

Fig 4.31 Comparison between [0°/90°]_s and [-45°/+45°]_s laminate, Third
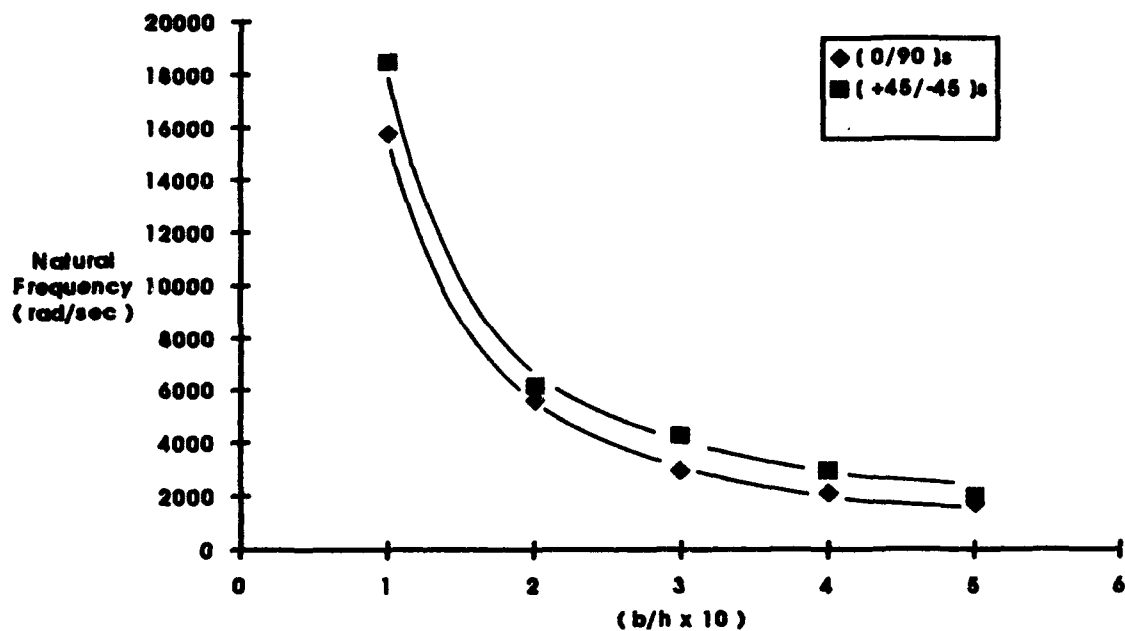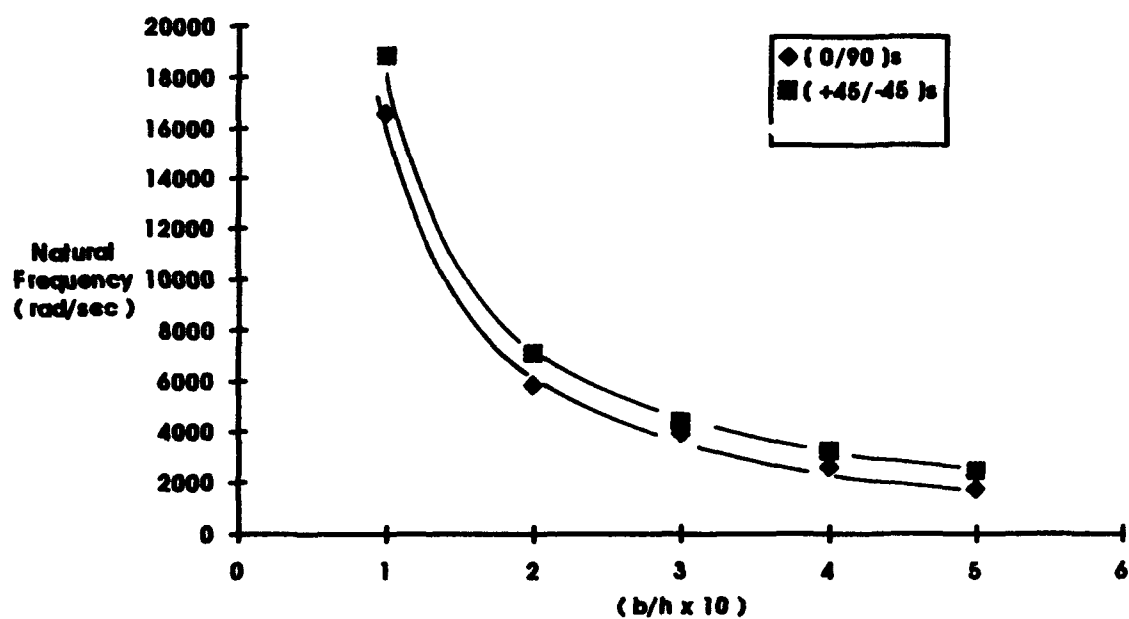Natural Frequency, Simply Supported-Free Boundary Condition

Fig 4.32 Comparison between [0°/90°]_s and [-45°/+45°]_s ply orientation,
Fourth Natural Frequency, Simply Supported-Free Boundary Condition

V. Conclusions and Recomendations

An analytical study was carried out using the DSHELL finite element program in the solution of dynamic response, natural frequencies and mode shapes, for curved Gr/Ep composite panels considering through the thickness shear strain.

Based upon on the analysis developed, the following conclusions were reached. Comparisons for a panel, used as a baseline study, with previous experimentation using Holographic Interferometry, and analytical studies using STAGSC-1 finite element code, proved to be excellent. The first four natural frequencies and the respective mode shapes obtained in this study matched completely with the results in the previous analysis.

It was found that modelling the composite shell panel was dictated by improving the accuracy of natural frequencies and mode shapes. The result from this was that four nodes have to be positioned per each half sine wave formed and the size of the subspace in the eigenvalue solution was fourteen vectors in arriving at the four eigenvalues requested.

Good results were obtained for a given panel, considering the two boundary conditions studied, all edges simply supported and simply supported-free. The output obtained from DSHELL was close to the results obtained from the Galerkin Technique. The accuracy and flexibility of the program was proved.

The curvature of the composite shells were varied as was the span to thickness ratio in order to measure the effects for each ply orientation, under the specified boundary

conditions. The results showed that, as the shell becomes deeper the frequency becomes smaller.

Findings show that larger curvature increases the natural frequencies for both laminates $[0^o/90^o]_S$ and $[-45^o/+45^o]_S$ due to the fact that the in-plane displacements (u and v specially) becomes more important as the curvature increases. This was found considering simply supported all around and simply supported-free boundary condition.

It was found also that the effect of through the thickness shear was more observable at the shallower end of the composite shell where the panel becomes thick ($\delta/h < 1$), but this effect disappears as the curvature effects becomes predominant.

Results show that shallow shell theory is a good approximation when the δ/c ratio is less than 0.25, but as the ratio increases the interaction of the in-plane displacements must be considered as part of the eigenvector-eigenvalue solution.

Appendix A: More Details Related to the Subspace Iteration Method

The purpose of this section is to present some additional details in the subspace method used in the DSHELL program.

A.1 Subspace Iteration Method

The subspace iteration algorithm was developed by Bathe [1] and is explained in this section. The goal of the subspace iteration method is to solve for the "p" lowest eigenvalues and eigenvectors which satisfy

$$K\Phi = M\Phi\Lambda \qquad\qquad (A.1)$$

where $\Phi = [\{ \Phi_1 \} \{ \Phi_2 \}....\{\Phi_p\}]$, $\Lambda = $ diag matrix of eigenvalues λ_i's (i = 1, 2, ...,p), and K and M are the symmetric stiffness and mass matrices respectively. The starting iterationvectors, x_1, span the subspace (eigensubspace)E_1 and iteration continues until, with sufficient accuracy, E_∞ is spanned. E_∞ is the p-dimensional subspace spanned by the "p" lowest eigenvectors. The starting iteration vectors should be chosen to excite those degrees of freedom possessing large mass and small stiffness [1:682]. One method for obtaining x_1, which has been effectively used, begins by letting the first column of [M]x_1 be the major diagonal of [M]. This establishes excitation of all degrees of freedom

possessing mass. The other columns of $[M]x_1$ are unit vectors with a "1" at locations with the smallest K_{ii}/m_{ii} ratios. Therefore, all locations but one within these columns contains zeros. The last column in $[M]x_1$ can be a random vector. After the starting iteration vector is determined, iteration begins from E_k to E_{k+1} (E_∞ is the eventual desired result), where $k = 1, 2, 3, ..., n$ by applying

$$K \bar{x}_{k+1} = M x_k \qquad (A.2)$$

As used here, "n" is the number of iterations required to obtained convergence. Equation (A.1) is solved for $\bar{x}_{k+1}$ by premultiplication of both sides of the equation by $[K]^{-1}$ to yield

$$\bar{x}_{k+1} = K^{-1} M x_k \qquad (A.3)$$

Next, the projections of the K and M operators on the E_{k+1} subspace are determined by [1]

$$K_{k+1} = \bar{x}^T_{k+1} \ K \bar{x}_{k+1} \qquad (A.4)$$

$$M_{k+1} = \bar{x}^T_{k+1} \ M \bar{x}_{k+1} \qquad (A.5)$$

By using the above relations for K_{k+1} and M_{k+1}, the eigensystem of the projected operators can be solved by [1]

$$K_{k+1} \ Q_{k+1} = M_{k+1} \ Q_{k+1} \ \Lambda_{k+1} \qquad (A.6)$$

Equation (A.5) represents the reduced eigenvalue problem for the E_{k+1} subspace and can

be solved by any popular technique (DSHELL uses Householder's Method followed by a

LR algorithm) to obtained values for Q_{k+1} and Λ_{k+1}. An improved approximation to the

eigenvectors is found from [1]

$$x_{k+1} = \bar{x}_{k+1} \, Q_{k+1} \qquad\qquad (\text{A.7})$$

This procedure is iterated until the desired convergence is obtained. This x_{k+1} is now

substituted into Equation (A.2) in place of x_k and the algorithm iterated until sufficient

convergence has been obtained. Figure A-1 presents a flow chart of the subspace

iteration algorithm incorporated in DSHELL. In subspace iteration, the iteration vectors

are ordered such that the vectors converging to $\phi_1, \phi_2, ..., \phi_p$ are stored as the first,

second, ..., p^{th} columns of x_{k+1}, respectively. As long as no vector contained within x_1

isorthogonal to any of the required eigenvectors, then as k tends to infinity, Λ_{k+1}

approaches to Λ (the required diagonal matrix of "p" eigenvalues) and x_{k+1} approaches

$[\phi]$ (the required column matrix of "p" eigenvectors) [1]
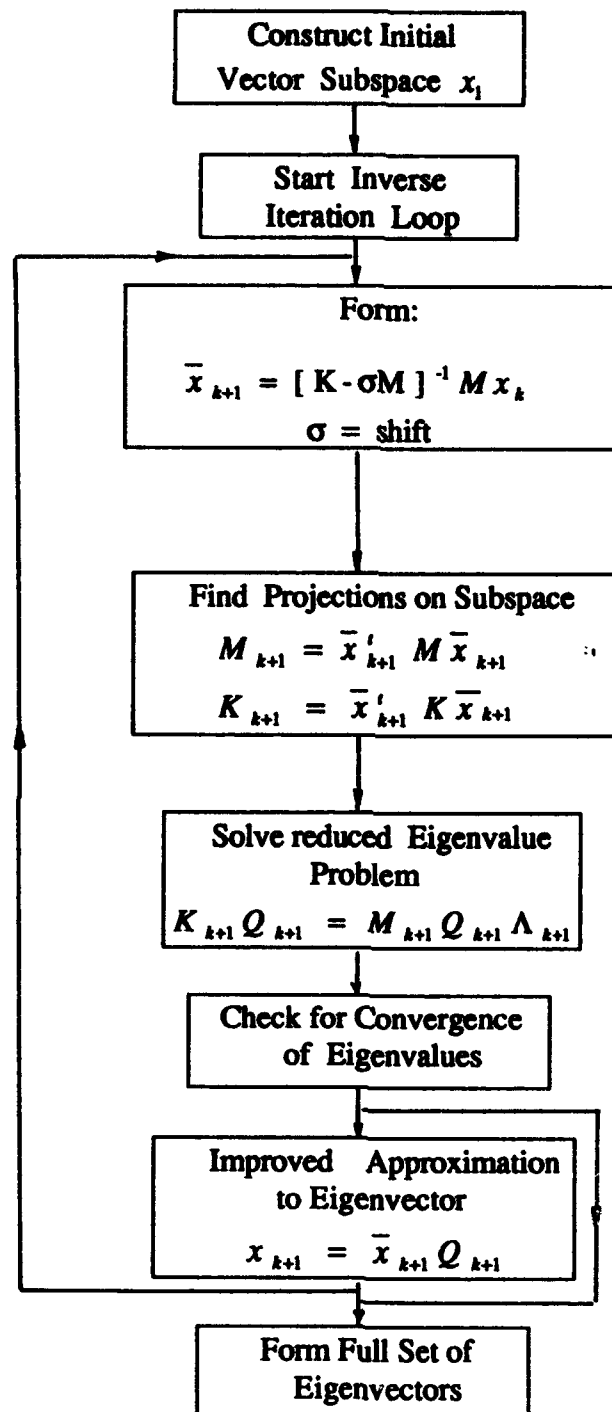
Fig A-1 Subspace Iteration Algorithm

Bibliography

1. Bathe, Klaus Jurgen. *Finite Element Procedures in Engineering Analysis.* New Jersey: Prentice-Hall Inc., 1982.

2. Bert, C.W., J.L.Baker and D.M.Egle. " Free Vibrations of Multilayer Anisotropic Cylindrical Shells," *Journal of Composite Materials.* Volume 3, No. , 480-499, July 1969.

3. Cook, Robert D. and others. *Concepts and Applications on Finite Element Analysis.* New York: John Wiley & Sons, 1989.

4. Cyr, Capt Garry J. *Effects of Cutout Orientation on Natural Frequencies and Mode Shapes of Curved Rectangular Composite Panels.* Master's Thesis, AFIT/GAE/AA/86D. School of Engineering, Air Force Institute of Technology, (AU), Wright-Patterson Air Force Base, Ohio, December 1986.

5. Cyr, G.J., R.L.Hinrichsen and R.A.Walley. " Effects of Cutouts on the Dynamic Response of Curved Rectangular Composite Panels, " *AIAA Journal,* Volume 26, No 5, 582-588, May, 1988.

6. Jones Robert M. *Mechanics of Composite Materials.* New York: Hemisphere Publishing Corporation, 1975.

7. Levraea, Jr. V.J., A.N. Palazotto and G.E. Maddux." The Effect of Cutout Positioning on the Dynamic Characteristics of a Curved Composite Panels," *Journal of Composite Structures.* Volume 23, 263-272, 1993.

8. Linneman, Capt Peter E. *Vibration and Buckling Characteristic of Composite Cylindrical Panels Incorporating the Effects of Higher Order Shear Theory.* MSc Thesis, AFIT/GA/AA/88D-06. School of Engineering, Air Force Institute of Technology, Wright-Patterson AFB OH, December 1988.

9. Maddux, Gene, Aerospace Engineer, *Flight Dynamic Laboratory,* Wright-Patterson AFB, OH. Personal Interview, April-May, 1994.

10. Meirovitch, Leonard. *Analytical Methods in Vibrations.* New York: The MacMillan Company, 1967.

11. Palazotto, A.N. and Dennis, Scott T., *Non Linear Analysis of Shells Structures.* Washington D.C.: American Institute of Aeronautics and Astronautics, Inc., 1992.

12. Palazotto, A.N. and Peter E. Linneman. " Vibration and Buckling Characteristics of Composites Cylindrical Panels Incorporating the Effects of a Higher Order Shear Theory," *International Journal of Engineering Sciences, 28 (3):* 341-361 (1991).

13. Reddy, J.N. *An Introduction to the Finite Element Method.* Second Edition. New York: McGraw-Hill., 1984.

14. Reddy, J.N. *Energy and Variational Methods in Applied Mechanics.* John Wiley & Sons, 1984

15. Saada, Adel S. *Elasticity: Theory and Applications.* New York: Pergamon Press, 1974.

16. Silva, K.J. *Finite Element Investigation of a Composite Cylindrical Shell Under Transverse Load with Through the Thickness Shear and Snapping.* M.S. Thesis, AFIT/GAE/ENY/89D-35. School of Engineering, Air Force Institute of Technology (AU), Wright-Patterson AFB, OH, 1989.

17. Smith, J. W. *Vibration of Structures: Applications in Civil Engineering Design.* London: Chapman and Hall, 1988.

18. Soedel, Werner. *Vibrations of Shells and Plates.* New York: Marcel Dekker, 1993.

19. Taylor Jr., Walter W., *Finite Element Investigation Into the Dynamic Inestability Characteristic of Laminated Composite Panels.* M.S. Thesis, AFIT/GAE/ENY/90D-28. School of Engineering, Air Force Institute of Technology (AU), Wright-Patterson AFB, OH, 1990.

20. Tighe, Kathleen V. and Palazotto A.N., " Higher Order Cylindrical Panel Relationships Considering General Ply Layups,". *Journal of Composite Structures.* Volume 27, 225-242, 1994.

21. Timoshenko, S., D.H. Young and W. Weaver Jr., *Vibration Problems in Engineering.* New York: John Wiley & Sons, 1974.

22. Tsai, C.T. and Palazotto A.N., "On the Finite Element Analysis of Non-Linear Vibration for Cylindrical Shells with Higher Order Shear Deformation Theory,". *International Journal of Non-Linear Mechanics, 26 No 3/4:* 379-388, (1991).

23. Vinson, Jack R. *The Behavior of Thin Walled Structures: Beams, Plates and Shells.* Dordrecht, The Netherlands: Kluwer Academic Publishers, 1989.

24. Walley, Capt Richard A. *Natural Frequencies and Mode Shapes of Curved Composite Panels with interior Cutouts*. Master's Thesis, AFIT/GAE/AA/85D-16. School of Engineering, Air Force Institute of Technology, (AU), Wright-Patterson Air Force Base, Ohio, December 1985.

25. Warlburton, G.B. *The Dynamic Behavior of Structures*. (Second Edition). Oxford: Pergamon Press, 1976.

Vita

José L. Monteverde E. was born on June 16, 1965 in Guayaquil, Ecuador. He graduated from high school in 1983 and attended the Escuela Superior Politécnica del Litoral from which he received his Bachelor of Science in Mechanical Engineering in September 1989. Upon graduation he was selected by the Ecuadorian Air Force for pursuing a Master's Degree in Aeronautical Engineering. He worked few months at Cotopaxi AFB as Maintenance Engineer before enrolling to AFIT. He entered the School of Engineering, Air Force Institute of Technology in June 1992.

Permanent Address

P.O.Box 09-01-5384
Guayaquil, Ecuador

REPORT DOCUMENTATION PAGE

Form Approved
OMB No. 0704-0188

1. AGENCY USE ONLY (Leave blank)	2. REPORT DATE 14 June 1994	3. REPORT TYPE AND DATES COVERED Master's Thesis

4. TITLE AND SUBTITLE
EFFECTS OF THICKNESS AND CURVATURE ON THE NATURAL
FREQUENCIES OF CYLINDRICAL COMPOSITE PANELS

5. FUNDING NUMBERS

6. AUTHOR(S)
Jose L Monteverde E
Ecuadorian Air Force

7. PERFORMING ORGANIZATION NAME(S) AND ADDRESS(ES)

Air Force Institute of Technology
WPAFB OH 45433-6583

8. PERFORMING ORGANIZATION REPORT NUMBER

AFIT/GAE/ENY/94J-2

9. SPONSORING/MONITORING AGENCY NAME(S) AND ADDRESS(ES)

Mr Arnold Mayer
Wright Laboratories (WL/FIB)
WPAFB OH 45433-5000

10. SPONSORING/MONITORING AGENCY REPORT NUMBER

11. SUPPLEMENTARY NOTES

12a. DISTRIBUTION/AVAILABILITY STATEMENT

Approved for public release; distribution unlimited

12b. DISTRIBUTION CODE

13. ABSTRACT (Maximum 200 words)

An analytical study is performed to determine the dynamic response, natural frequencies and mode shapes, of deep composite cylindrical shells, including the effects of through the thickness shear strain. The DSHELL finite element program is used to predict the first four natural frequencies and the results are compared to a reference using the Galerkin technique. The program was extended to problems considering simply supported-free boundary conditions. The mode shapes are created by plotting a surface-contour plot of the eigenvector vector output from DSHELL. A linear free vibration analysis is performed on two graphite/epoxy panels. These panels have different ply orientation. Comparisons between the first panel (used as a baseline) using DSHELL, with previous analytical and experimentation studies were found to correlate well. For the second panel, the curvature and the span to thickness ratio were varied in order to measure effects on two ply orientations: $[0°/90°]_s$ and $[-45°/+45°]_s$, under two boundary conditions. The results showed that, as the shell becomes deeper, the frequency becomes smaller. Also as the curvature increases, the frequencies increase.

14. SUBJECT TERMS
Linear Dynamics, Eigenvalue-Eigenvector, Finite Element
Analysis, Shells, Structural Mechanics, Composite materials,
Numerical Methods

15. NUMBER OF PAGES
98

16. PRICE CODE

17. SECURITY CLASSIFICATION OF REPORT Unclassified	18. SECURITY CLASSIFICATION OF THIS PAGE Unclassified	19. SECURITY CLASSIFICATION OF ABSTRACT Unclassified	20. LIMITATION OF ABSTRACT UL